5. Dynamics of Fibre Processing Processes

5.1 Dynamics of the Fibre Transport

5.1.1 Task

Each fibre manufacture and processing process is connected to the dynamic basic principle of the transport. Neither fibre formation nor fibre processing are possible without continuously running down transport operations, which are realised as a rule, by means of rotations for specific machine tools. Fibres or yarns are not able to pick up axial pressure forces. Therefore, a continuous fibre transport is only possible if a tensile force is produced and permanently maintained in the transported fibre or yarn. A controlled refining of the yarn (for instance in the draw process of man-made fibres) can even be effected by means of this tensile force besides the pure transport and processing (for instance twisting, package winding, sectional warping, texturing). On the one hand, specially man-made fibres are very sensitive to tensile force fluctuations during their processing. On the other, some disturbed process and product variables (caused for instance by thread guide elements, preparation oils, unbalanced machine tools, fluctuating fibre material itself) permanently influence the quantity of the tensile force. It is obvious that the dynamic analysis and the dynamic modelling of the basic process fibre transport is from fundamental and primary importance for the process analysis of the technological fibre formation and processing processes.
Some elaborated model ideas to this set of problems are presented in the following. These are valid for small deformation ranges (elongation demand $< 10\%$) in which current linearity is between tensile force and elongation in the first approximation. Nonlinear deformation processes (with changing fibre deformation characteristics along the fibre length or with essential plastic deformation parts) are excluded.
The investigations can be used as a basis for the treatment of the following problems:

- *process synthesis oriented* (for instance statements to favourable or unfavourable arrangement and design of machine tools in the thread line),
- *process analysis oriented* (for instance influence of thread guide elements to the thread unevenness, reaction of measuring sensors to the thread) or even

- *thread test oriented* (for instance questions in relationship with the frictional test or with the unevenness measuring of threads).

Besides our own detailed paper to fibre transport modelling [291] the reader should be referred to the complementing three papers dealing with the problem of running elastic fabrics between driven rolls [292]- [294]; [295] is also recommended.
The analysis of any continuous running thread line in a fibre formation, fibre processing or fibre testing machine or apparatus shows that three different thread strain lines (arranged in different manners of series) can be found: These are the *delay thread line*, the *dead time thread line* and the *friction thread line*.
The dynamic modelling of any realised thread transport process therefore supposes knowledge and solutions of the dynamic description equations (that means the DEq.) for the three named typical thread transport strain lines.

5.1.2 Dynamic Model to the Description of a Delay Thread Line

A *delay thread line* is in the present relationship a part of a transported, under a tensile force situated, thread with the length l which runs into this part with the velocity v_i and the fineness Tt_i and comes out of this part with the velocity v_o and the fineness Tt_o. Here: $v_\mathrm{o} > v_\mathrm{i}$ (trivial condition for the improvement of a tensile force) is valid and each fineness change comes off evenly at each point along this part. The last prerequisite is a simplification for the transported thread in the settled limited strain range which the thread attributed rubber elastic behaviour.

Figure 5.1 (already known in a similar form, compare Figs. 2.5 and 4.20) shows a possible practical realisation for the given definition. At this, one can also imagine, the backing-off point of a thread from a cop which is transported along a determined free way distance into the rotating input element of a thread processing machine.

The linearised DEq. (the mathematical dynamic model) of such a delay thread line can be deduced naturally from the basic Eqs. 2.23 and 4.7 to:

$$(v_\mathrm{om}+p\cdot l_\mathrm{m})\cdot\Delta Tt_\mathrm{o}+Tt_\mathrm{om}\cdot\Delta v_\mathrm{o}-v_\mathrm{im}\cdot\Delta Tt_\mathrm{i}-Tt_\mathrm{im}\cdot\Delta v_\mathrm{i}+p\cdot Tt_\mathrm{om}\cdot\Delta l=0 \qquad (5.1)$$

Equation 5.1 can be transmitted easily to the dynamic transfer function (repeatedly explained in Chap. 4 before) from which all further dynamic functions in the frequency and time range are calculable.
It is easy to state that after some practice in the handling of DEqs. in the operator style of writing and their solution functions that the dynamic behaviour of a delay thread line is practically identical to the already fully described behaviour of the fibre formation distance in melt spinning polymers for the product variable fibre fineness (see also Sect. 4.2.1). All resulting equations and their normalised presentations (Figs. 4.4 to 4.6) are valid, similarly, for the transport delay line. It is simple to substitute the variables q_i, q_im and Δq_i

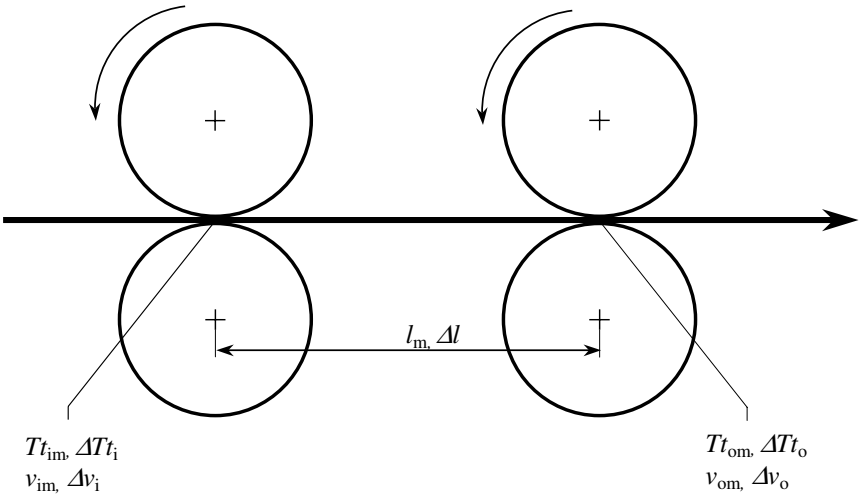

Fig. 5.1. Technological scheme of a delay thread line

by Tt_{i}, Tt_{im} and ΔTt_{i} in Sect. 4.2.1. $\Delta\varrho = 0$ is to be set additionally because this variable is not of interest here.

In the following practical example of Sect. 5.1.5 we will fall back upon Eq. 5.1 and its application will be demonstrated.

5.1.3 Dynamic Model to the Description of a Dead Time Thread Line

A *dead time thread line* is in the present relationship a part of a transported, under a tensile force situated, thread with the length l which runs into this part with the velocity v_{i} and the fineness Tt_{i} and comes out of this part with the velocity v_{o} and the fineness Tt_{o}. Here: $v_{\mathrm{o}} = v_{\mathrm{i}}$ is valid and the thread does not suffer fineness changes inside this part.
This definition says that the input thread fineness appears unchanged at the output after running through this part (after the so-called dead time T_{d} has expired). Under this condition:
mass inflow per time $=$ $Tt_{\mathrm{i}} \cdot v_{\mathrm{i}}$
mass discharge per time $=$ $Tt_{\mathrm{o}} \cdot v_{\mathrm{o}}$
with the both boundary conditions

$$v_{\mathrm{o}} = v_{\mathrm{i}} \tag{5.2}$$

$$Tt_{\mathrm{o}} = Tt_{\mathrm{i}} \cdot \exp(-p \cdot T_{\mathrm{d}}) \tag{5.3}$$

Figure 5.2 shows a realisation of a thread (transport) dead time line. Equation 5.3 expresses the dead time relation between Tt_{o} and Tt_{i} in the

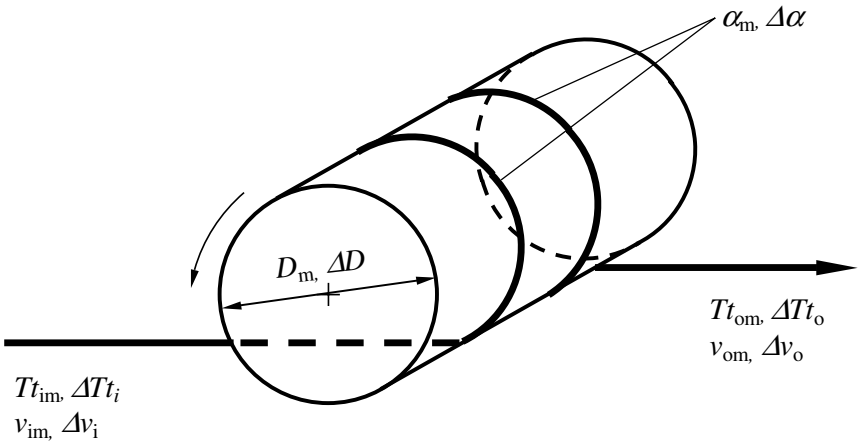

Fig. 5.2. Technological scheme of a dead time thread line

style of operator writing. It is the dynamic transfer equation for dead time elements known from the automatic control engineering (see for instance [10]). If the dead time T_d is realised by the thread wrap around a cylindrical thread transport element (for instance a wrapped godet which is a typical dead time transport element) with the diameter D, the angle of wrap α (in radian measure) and the circumference velocity v_i can then be written as:

$$T_d = \frac{D \cdot \alpha}{2 \cdot v_i} \tag{5.4}$$

One gets the dynamic model equation (first of all nonlinearly according to the variables Tt_i, Tt_o, v_i, D and α) for the dead time thread line by putting Eq. 5.4 into 5.3:

$$\Phi = Tt_o - Tt_i \cdot \exp\left(-p \cdot \frac{D \cdot \alpha}{2 \cdot v_i}\right) = 0 \tag{5.5}$$

Linearisation by means of partial differentiation then results in the linearised final motion DEq. of the dead time thread line to:

$$\begin{aligned}
&\Delta Tt_o - \exp\left(-p \cdot \frac{D_m \cdot \alpha_m}{2 \cdot v_{im}}\right) \cdot \Delta Tt_i \\
&-p \cdot \frac{Tt_{im} \cdot D_m \cdot \alpha_m}{2 \cdot v_{im}^2} \cdot \exp\left(-p \cdot \frac{D_m \cdot \alpha_m}{2 \cdot v_{im}}\right) \cdot \Delta v_i \\
&+p \cdot \frac{Tt_{im} \cdot \alpha_m}{2 \cdot v_{im}} \cdot \exp\left(-p \cdot \frac{D_m \cdot \alpha_m}{2 \cdot v_{im}}\right) \cdot \Delta D \\
&+p \cdot \frac{Tt_{im} \cdot D_m}{2 \cdot v_{im}} \cdot \exp\left(-p \cdot \frac{D_m \cdot \alpha_m}{2 \cdot v_{im}}\right) \cdot \Delta\alpha = 0
\end{aligned}$$

(5.6)

Equation 5.6 can be transmitted into the, in each case interesting, dynamic transfer function for determined concrete cause-effect-questions. From the latter the frequency, the amplitude and the phase frequency responses are calculable. The effect variable output thread fineness Tt_o will surely be of special interest in most cases. It is to be remarked that the calculation of the step response on the basis of the transfer function (by means of the residue theorem of the LAPLACE-transformation) is not possible here because the step response function of a dead time thread line is not a continuous function. The practical application of Eq. 5.6 will be demonstrated by means of an example in Sect. 5.1.5.

5.1.4 Dynamic Model to the Description of a Friction Thread Line

A *friction thread line* is in the present relationship a part of a transported, under a tensile force situated, thread with the length l which runs into this part with the velocity v_i and the fineness Tt_i and comes out of this part with the velocity v_o and the fineness Tt_o. Thus the following statement is valid: The tensile force of the thread increases permanently along the part according to the tensile friction law and the thread fineness decreases (a constant E-modulus of the thread material is presumed) permanently according to the same law (in a modified manner).
Friction lines appear practically on all fixed thread guides at the thread transport. They are as you know even consciously designed parts of the appropriate friction test apparatuses. The technological scheme of such a friction thread line is shown in Fig. 5.3. It is at first necessary to determine the thread mass on the friction element to the development of the continuity equation for the dynamic working case. The following is valid for the tensile force in the input and output thread (F_i and F_o):

$$F_o = F_i \cdot e^{\mu \cdot \alpha} \tag{5.7}$$

$e^{\mu \cdot \alpha}$ rope friction factor
μ coefficient of friction
α angle of wrap (in radian measure)

The tensile force within a thread (which possesses the fineness Tt_{zm} before the force influence on it and the fineness Tt_i during the force influence on it) can be written as:

$$F_i = A_{zm} \cdot Tt_{zm} \left[\frac{Tt_{zm}}{Tt_i} - 1 \right] \tag{5.8}$$

A_{zm} to the thread fineness related rise of the force-elongation-curve of the thread; dimension: force $\cdot$ fineness^{-1} $\cdot$ (relative length change)$^{-1}$

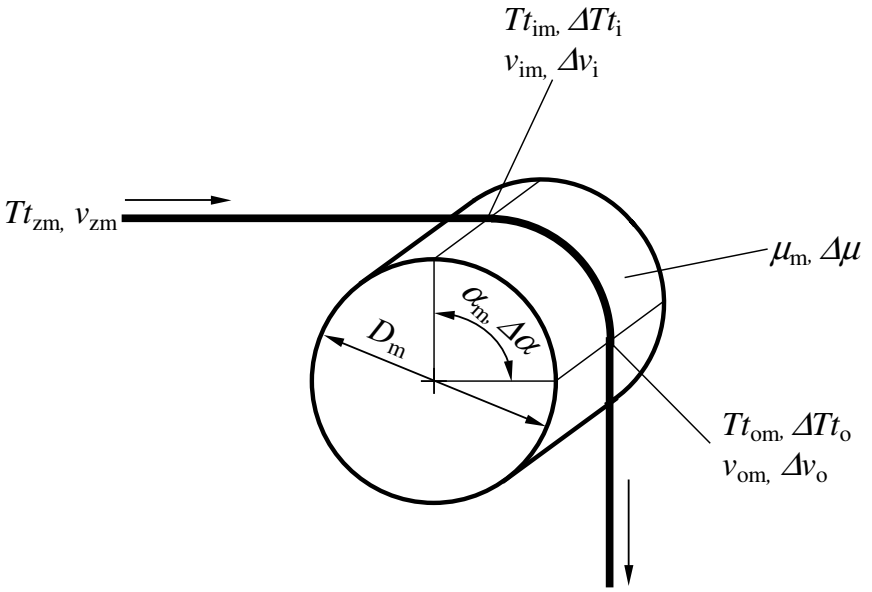

Fig. 5.3. Technological scheme of a friction thread line

Equation 5.8 put in Eq. 5.7 results:

$$A_{zm} \cdot Tt_{zm} \left[\frac{Tt_{zm}}{Tt_o} - 1 \right] = A_{zm} \cdot Tt_{zm} \left[\frac{Tt_{zm}}{Tt_i} - 1 \right] \cdot \exp(\mu \cdot \alpha) \tag{5.9}$$

Equation 5.9 results for Tt_o:

$$Tt_o = \frac{Tt_{zm}}{\left[\frac{Tt_{zm}}{Tt_i} - 1 \right] \cdot \exp(\mu \cdot \alpha) + 1} \tag{5.10}$$

The, on the friction element situated, thread mass M can now be determined by means of Eq. 5.10. The fineness Tt_o (dependent on the angle of wrap α) is to be multiplied by the circular arc $\alpha \cdot D_m/2$ to this (D_m = diameter of the friction element). Because T_o is a function of α it is to be integrated over the whole way of friction:

$$M = \frac{D_m}{2} \int_o^\alpha \frac{Tt_{zm}}{\left[\frac{Tt_{zm}}{Tt_i} - 1 \right] \cdot \exp(\mu \cdot \alpha) + 1} \cdot d\alpha \tag{5.11}$$

The solution of Eq. 5.11 results after substitution:

$$M = \frac{D_m \cdot Tt_{zm}}{2 \cdot \mu} \left\{ \mu \cdot \alpha + \ln \frac{\left[\frac{Tt_{zm}}{Tt_i} - 1 \right] + 1}{\left[\frac{Tt_{zm}}{Tt_i} - 1 \right] \cdot \exp(\mu \cdot \alpha) + 1} \right\} \tag{5.12}$$

If Eq. 5.10 is reduced to Tt_i and this value is inserted in Eq. 5.12 then one gets the thread mass on the friction element M in dependent upon the output thread fineness Tt_o:

$$M = \frac{D_\mathrm{m} \cdot Tt_\mathrm{zm}}{2 \cdot \mu} \left[\mu \cdot \alpha + \ln \frac{(Tt_\mathrm{zm} - Tt_\mathrm{o}) \cdot \exp(-\mu \cdot \alpha) + Tt_\mathrm{o}}{Tt_\mathrm{zm}} \right] \tag{5.13}$$

The time differential of Eq. 5.13 can be formed now because the value $\mathrm{d}m/\mathrm{d}t$ is nothing else than the changing thread mass on the friction element if Tt_o changes. This change element is easy to calculate:

$$\frac{\mathrm{d}M}{\mathrm{d}t} = \frac{D_\mathrm{m} \cdot Tt_\mathrm{zm}[1 - \exp(-\mu \cdot \alpha)]}{2 \cdot \mu (Tt_\mathrm{zm} - Tt_\mathrm{o}) \cdot \exp(-\mu \cdot \alpha) + Tt_\mathrm{o}} \cdot \dot{T}t_\mathrm{o} \tag{5.14}$$

Equation 5.14 represents the change of stored mass. The nonlinear DEq. as the dynamic model equation for a friction thread line according to the basic Eq. 2.23 can now be written with the latter and both quantities

- mass inflow per time $= Tt_\mathrm{i} \cdot v_\mathrm{i}$ and
- mass discharge per time $= Tt_\mathrm{o} \cdot v_\mathrm{o}$

$$\Phi = v_\mathrm{o} \cdot Tt_\mathrm{o} + \frac{\mathrm{d}M}{\mathrm{d}t} = \frac{D_\mathrm{m} \cdot Tt_\mathrm{zm}[1 - \exp(-\mu \cdot \alpha)]}{2 \cdot \mu (Tt_\mathrm{zm} - Tt_\mathrm{o}) \cdot \exp(-\mu \cdot \alpha) + Tt_\mathrm{o}} \cdot Tt_\mathrm{o} \cdot p - v_\mathrm{i} \cdot Tt_\mathrm{i} = 0 \tag{5.15}$$

After partial derivation to all quantities which can change (v_o, v_i, Tt_o, Tt_i, μ, α) the following linearised motion-DEq. for a friction thread line results from Eq. 5.15:

$$\begin{aligned}
&Tt_\mathrm{om} \cdot \Delta v_\mathrm{o} - Tt_\mathrm{im} \cdot \Delta v_\mathrm{i} - v_\mathrm{im} \cdot \Delta Tt_\mathrm{i} \\
&+ \left\{ v_\mathrm{om} + p \frac{2Tt_\mathrm{zm}^2 D_\mathrm{m} \mu_\mathrm{m} \exp(-\mu_\mathrm{m}\alpha_\mathrm{m})[1 - \exp(-\mu_\mathrm{m}\alpha_\mathrm{m})]}{[2\mu_\mathrm{m}(Tt_\mathrm{zm} - Tt_\mathrm{om})\exp(-\mu_\mathrm{m}\alpha_\mathrm{m}) + Tt_\mathrm{om}]^2} \right\} \cdot \Delta Tt_\mathrm{o} \\
&+ p \frac{2Tt_\mathrm{zm} Tt_\mathrm{om} D_\mathrm{m} \exp(-\mu_\mathrm{m}\alpha_\mathrm{m})[Tt_\mathrm{om}\alpha_\mathrm{m}/2 - (Tt_\mathrm{zm} - Tt_\mathrm{om})[\mu_\mathrm{m}\alpha_\mathrm{m} - \exp(-\mu_\mathrm{m}\alpha_\mathrm{m})]]}{[2\mu_\mathrm{m}(Tt_\mathrm{zm} - Tt_\mathrm{om})\exp(-\mu_\mathrm{m}\alpha_\mathrm{m}) + Tt_\mathrm{om}]^2} \cdot \Delta\mu \\
&+ p \frac{2Tt_\mathrm{zm} Tt_\mathrm{om} D_\mathrm{m} \mu_\mathrm{m} \exp(-\mu_\mathrm{m}\alpha_\mathrm{m})[Tt_\mathrm{om}/2 + \mu_\mathrm{m}(Tt_\mathrm{zm} - Tt_\mathrm{om})]}{[2\mu_\mathrm{m}(Tt_\mathrm{zm} - Tt_\mathrm{om})\exp(-\mu_\mathrm{m}\alpha_\mathrm{m}) + Tt_\mathrm{om}]^2} \cdot \Delta\alpha = 0
\end{aligned} \tag{5.16}$$

The structure of Eq. 5.16 is a bit more complicated than the derivated equations until now. Nevertheless, it is the basis of the dynamic transfer functions and their derivated functions in the frequency range (frequency, amplitude, and phase frequency responses) which can answer to appointed cause-effect-questions. In the following subsection the use of the dynamic model Eqs. 5.1, 5.6 and 5.16 of the delay, dead time and friction lines thread will be represented by means of some practical examples. From these derived statements it will also be shown for the carrying out of the process.

5.1.5 Examples of Quantitative Investigations of Fibre Transport Processes

Fibre Influence in a Series Arrangement of Delay and Dead Time Thread Lines

The investigated delay thread line with a following dead time thread line is shown in Fig. 5.4. A practical realisation could be, for instance, that the thread runs from a supply bobbin into the manifold wrapped taking in godet of a drawing zone or the thread runs in an elongation zone realised between a taking in godet and a manifold wrapped taking out godet.

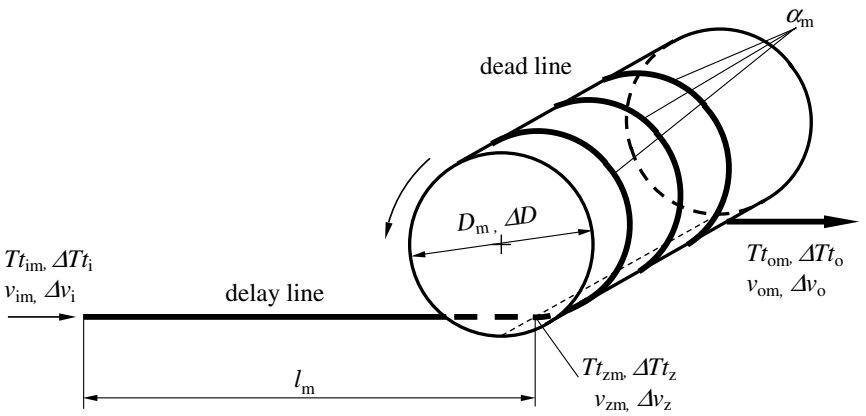

Fig. 5.4. Series arrangement of a delay and a dead time thread line

The used abbreviations mean:

Tt_{im}, v_{im}	mean value of the thread fineness or velocity at the input into the delay line
ΔTt_{i}, Δv_{i}	changes of the thread fineness or velocity around their mean values at the input into the delay line
Tt_{zm}, v_{zm}	mean value of the thread fineness or velocity at input into the dead time line ($\equiv$ output of the delay line)
ΔTt_{z}, Δv_{z}	changes of the thread fineness or velocity around their mean values at input into the dead time thread line ($\equiv$ output of the delay line)
Tt_{om}, v_{om}	mean value of the thread fineness or velocity at output of the dead time line
ΔTt_{o}, Δv_{o}	changes of the thread fineness or velocity around their mean values at output of the dead time line
l_{m}	length of the delay line
D_{m}	diameter of the godet
ΔD	change of the godet diameter
α_{m}	angle of wrap of the thread around the godet (in radian measure)

The dynamic model equations of a delay thread line (Eq. 5.1) and a dead time thread line (Eq. 5.6) – applied to the present case – are used for the calculation of the dynamic transfer function for a cause-effect relation whose aim is also to be defined. It should be assumed that ΔD (no eccentricity of the godet) as well as Δv_z and Δv_o (no speed changes of the transport godet) and ΔTt_i (no changes of the input thread fineness) are equal to zero. Moreover, if it is considered that $v_\mathrm{zm} = v_\mathrm{om}$ and $Tt_\mathrm{zm} = Tt_\mathrm{om}$ then the equations can be written as
delay line

$$(v_\mathrm{om} + p \cdot l_\mathrm{m}) \cdot \Delta Tt_\mathrm{z} - Tt_\mathrm{im} \cdot \Delta v_\mathrm{i} = 0 \tag{5.17}$$

dead time line

$$\Delta Tt_\mathrm{o} - \exp\left(-p \cdot \frac{D_\mathrm{m} \cdot \alpha_\mathrm{m}}{2 \cdot v_\mathrm{om}}\right) \cdot \Delta Tt_\mathrm{z} = 0 \tag{5.18}$$

It should now be investigated whether the reactions of the fineness at the output of the transport godet (ΔTt_o) are if the velocity is changing at the input of the whole transport line (Δv_i). Now the *dynamic transfer function* is to be formed

$$G(p) = \frac{\Delta Tt_\mathrm{o}}{\Delta v_\mathrm{i}}$$

which is to be calculated from Eqs. 5.17 and 5.18 as follows:

$$G(p) = \frac{\Delta Tt_\mathrm{o}}{\Delta v_\mathrm{i}} = \frac{Tt_\mathrm{im}}{v_\mathrm{om}} \cdot \frac{\exp\left(-p \cdot \dfrac{D_\mathrm{m} \cdot \alpha_\mathrm{m}}{2 \cdot v_\mathrm{om}}\right)}{1 + p \cdot \dfrac{l_\mathrm{m}}{v_\mathrm{om}}} \tag{5.19}$$

amplitude frequency response

$$|G(\mathrm{j}f)| = \left| \frac{\widetilde{\Delta Tt_\mathrm{o}}}{\widetilde{\Delta v_\mathrm{i}}} \right| = \frac{Tt_\mathrm{im}}{\sqrt{v_\mathrm{om}^2 + (2\pi f \cdot l_\mathrm{m})^2}} \tag{5.20}$$

phase frequency response

$$\varphi(f) = \arctan\left[-\frac{2\pi f \cdot l_\mathrm{m} \cdot \cos\left(\dfrac{D_\mathrm{m}\alpha_\mathrm{m}\pi}{v_\mathrm{om}} \cdot f\right) + v_\mathrm{om} \cdot \sin\left(\dfrac{D_\mathrm{m}\alpha_\mathrm{m}\pi}{v_\mathrm{om}} \cdot f\right)}{v_\mathrm{om} \cdot \cos\left(\dfrac{D_\mathrm{m}\alpha_\mathrm{m}\pi}{v_\mathrm{om}} \cdot f\right) - 2\pi f \cdot l_\mathrm{m} \cdot \sin\left(\dfrac{D_\mathrm{m}\alpha_\mathrm{m}\pi}{v_\mathrm{om}} \cdot f\right)} \right] \tag{5.21}$$

The phase shift angle $\varphi(f)$ (Eq. 5.21) indicates (as you know) in which angle φ (related to a full cycle duration of the disturbance oscillation) the effect-oscillation follows the cause-(disturbance-)oscillation. It is easily possible to conclude from this phase shift angle $\varphi(f)$ by means of the known output velocity v_{om} and of Eq. 2.50 to the thread length L_{d} which passes the transport system at its output before an input disturbance reaches this output. An independent representation of this delay thread length L_{d} from the velocity v_{om} can be given if it does not use the disturbance frequency f as an independent variable, but the wavelength λ_{f} of a full cycle duration of the disturbance in the thread. It is connected with the disturbance frequency f and the thread output velocity v_{om} according to the relation

$$f = \frac{v_{\mathrm{om}}}{\lambda_{\mathrm{f}}} \tag{5.22}$$

Comparable to this is also the equivalent Eq. 4.57.

The nomogram Fig. 5.5 should be inserted at this point. It allows the conversion of the single quantities into each other and it can be used because it is generally valid for other interests of the same kind which are presented for instance in the Sects. 4.3.3, 4.4.2, 4.4.3 and the Sect. 4.5.

The amplitude frequency response of Eq. 5.20 and the delay thread length L_{d} are represented in Figs. 5.6 and 5.7 depending upon the disturbance frequency f and of the correlated thread length (in connection with the thread output velocity), which represents a full disturbance oscillation. The corresponding dependences are epitomised presented for the following process and product variables (only for v_{im}=100 m/min) relating to the model arrangement in Fig. 5.4:

Tt_{im} = 3.4 tex
Tt_{om} = 3.3 tex
D_{m} = 0.1 m, 0.2 m
α_{m} = 0 (thread goes out the delay thread line directly)
α_{m} = 2π, 6π, 10π ($\equiv$ 1, 3, 5 wraps round the godet)
l_{m} = 0.5 m, 1.0 m, 2.0 m
v_{im} = 100 m/min, 500 m/min, 1000 m/min
v_{om} = 103 m/min, 515 m/min, 1030 m/min

The following statements are to be derived also concerning the not presented results of the higher thread velocities:

a) The amplitude frequency responses (Fig. 5.6) show that the amplitude of the output fineness change $\widetilde{\Delta Tt_{\mathrm{o}}}$ (caused by an input disturbance of the velocity $\widetilde{\Delta v_{\mathrm{i}}}$) is independent on it, if a dead time thread line of any length follows to the delay thread line or not. The result means that the imprinted

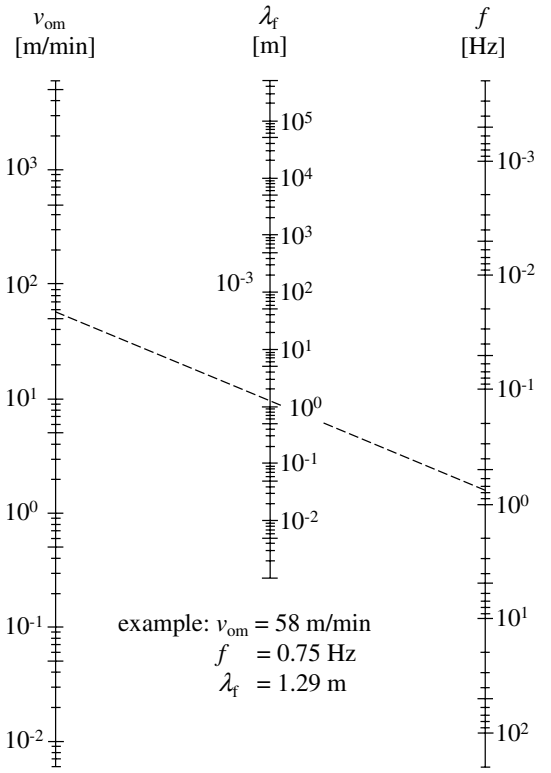

Fig. 5.5. Nomogram to the estimation of the relationship between the thread velocity v_{om}, the disturbance frequency f and the disturbance wavelength λ_f

thread fineness changes $\widetilde{\Delta T t_o}$ along a godet line with more or less wraps will neither decrease nor increase. They appear at the output unchanged and are only delayed by the pure transport time (see definition of the dead time in the Sect. 5.1.3).

b) Disturbances of the input velocity $\widetilde{\Delta v_i}$ of ≥ 50 m/min (according to a frequency of the disturbance f of $\leq 3.3 \cdot 10^{-2}$ Hz at $v_{im} = 100$ m/min or $\leq 3.3 \cdot 10^{-1}$ Hz at $v_{im} = 1000$ m/min) will be transmitted practically undamped to the output thread fineness $T t_o$.

c) A practical complete dampening is reached if the disturbance is ≤ 50 mm (according to a frequency of the disturbance f of ≥ 33 Hz at $v_{im} = 100$ m/min or ≥ 330 Hz at $v_{im} = 1000$ m/min). It is furthermore to read that the dampening effect is already put in at smaller frequencies the greater the length of the delay line.

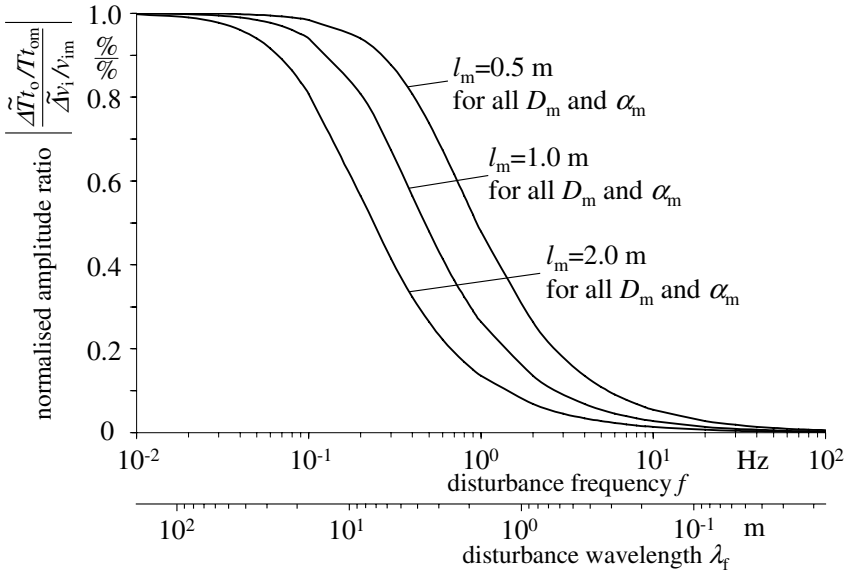

Fig. 5.6. Normalised amplitude frequency responses of fineness changes $\widetilde{\Delta T t_o}$ caused by input velocity changes $\widetilde{\Delta v_i}$ after the thread line arrangement Fig. 5.4, input velocity $v_{im} = 100$ m/min

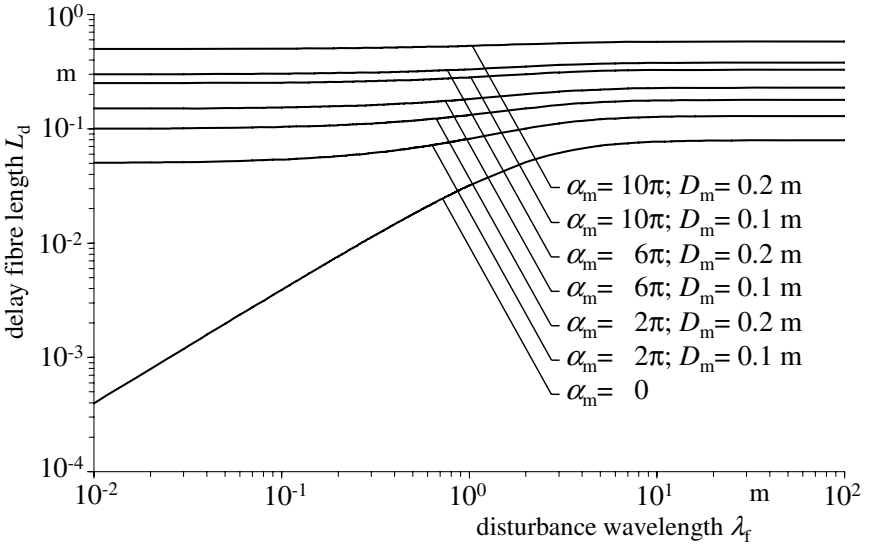

Fig. 5.7. Delay fibre length L_d, length of the delay thread line $l_m = 0.5$ m, thread line arrangement after Fig. 5.4

d) It is furthermore remarkable that a variation of the delay thread line length lowers or raises the critical frequencies in a similar ratio. From this it is derivable that the dampening of such input velocity disturbances is better the longer the line can be selected from the thread unwinding point to the machine input. Such disturbances happen for instance at the twisting, draw twisting or knitting in form of so-called "thread plucks" or also in longer periodic unwinding fluctuations by means of oil fluctuations on the thread. An extension of this line alone must also work for thread break behaviour, because the thread break is an extreme case of fineness change ($\Delta Tt = -Tt_{\mathrm{m}}$). Each measurement must effect diminishing, to the thread breaks, which fineness changes damp or dismantle, indifferent of which cause is produced.

e) The knowledge of the delay thread length L_{d} is also important for the cause research of unevennesses (Fig. 5.7). The dead times (caused by different roll wraps and diameters) are of decisive influence on L_{d} (contrary to the amplitude frequency response) specifically in the disturbance wavelength range ≤ 1 m. Whereas the delay thread length L_{d} with missing dead time ($\alpha_{\mathrm{m}} = 0$) line increases very strongly with increasing disturbance wavelength λ_{f} (according to decreasing disturbance frequency f, notice the double logarithm axes in Fig. 5.7) the dependence on the disturbance wavelength decreases with the increasing dead time line. The delay thread length L_{d} approaches a limit value versus the disturbance wavelength λ_{f} which is exactly equivalent to the length of the delay thread line l_{m}. This behaviour means practically that L_{d} is determined for $\lambda_{\mathrm{f}} \leq 1$ m (according to great disturbance frequencies f) almost fully by the dead time thread line, whereas the influence of the delay thread line (according to the length of this) will be relatively stronger for great disturbance wavelengths $\lambda_{\mathrm{f}} \geq 5$ m (according to small disturbance frequencies f).

f) The relationships show that specific short-time disturbances of high frequencies (with short and shortest wavelengths) in the thread (they influence the thread break behaviour especially drasticly) are very difficult to characterise only by their cause-effect relationship. The reason is that their amplitudes are probably strongly dampened (specifically for long delay lines) and because (specifically for short delay lines) the delay thread length L_{d} can amount to the multiple of the disturbance wavelength λ_{f}.

It is absolutely necessary that dynamic model investigations be carried out for such practical interesting cases to the design of unique relationships out of dynamic measurements. It can also be necessary that the interpretation of the measuring results be found by cross-correlation analysis of the disturbance time functions and their effects to the thread fineness (see to this Chap. 6).

Fibre Influence at Fixed Thread Guides (Friction Thread Lines)

The thread line at fixed thread guides (thread deflection elements, thread guides, friction brakes) has been defined as the friction line. The already used scheme of the thread guidance around a fixed friction element (Fig. 5.3) will be investigated quantitatively in the following more throughly. The used symbols of the dynamic model Eq. 5.16 and their meaning should be given as:

Tt_{zm}, v_{zm}	mean values of the thread fineness or velocity of the tensionless thread
Tt_{im}, v_{im}	mean values of the thread fineness or velocity at the input into the friction thread line
Tt_{om}, v_{om}	mean values of the thread fineness or velocity at the output of the friction thread line
D_{m}	diameter of the fixed (friction) thread guide
α_{m}	mean value of the angle of wrap of the thread around the fixed (friction) thread guide (in radian measure)
μ_{m}	mean value of the friction coefficient thread-thread guide
$\Delta Tt_{\mathrm{i}}, \Delta Tt_{\mathrm{o}}, \Delta v_{\mathrm{i}}, \Delta v_{\mathrm{o}}, \Delta\mu_{\mathrm{m}}, \Delta\alpha_{\mathrm{m}}, \Delta D$	changes of the adequate sizes around their mean values

It is assumed according to Eq. 5.16 that D, Tt_{z}, v_{z}, v_{o} and α are constant (the appropriate possible changes ΔD, ΔTt_{z}, Δv_{z}, Δv_{o} and $\Delta\alpha$ are assumed to be zero). Equation 5.16 is simplified appropriately then.

It is investigated in the following how the fineness change ΔTt_{o} acts if either the velocity at the input of the friction thread line v_{i} or the friction coefficient μ fluctuate. The fineness of the thread at the input should be constant ($\Delta Tt_{\mathrm{i}} = 0$).

The *amplitude frequency responses* for the named disturbances are:

$$|G(\mathrm{j}f)| = \left| \frac{\widetilde{\Delta Tt_{\mathrm{o}}}}{\widetilde{\Delta v_{\mathrm{i}}}} \right| = \frac{Tt_{\mathrm{im}} \cdot A_{\mathrm{a}}}{\sqrt{A_{\mathrm{a}}^2 \cdot B_{\mathrm{a}}^2 + (2\pi f \cdot C_{\mathrm{a}})^2}} \tag{5.23}$$

$$|G(\mathrm{j}f)| = \left| \frac{\widetilde{\Delta Tt_{\mathrm{o}}}}{\widetilde{\Delta\mu}} \right| = \frac{2\pi f \cdot E_{\mathrm{a}}}{\sqrt{A_{\mathrm{a}}^2 \cdot B_{\mathrm{a}}^2 + (2\pi f \cdot C_{\mathrm{a}})^2}} \tag{5.24}$$

with the abbreviations

$$A_{\mathrm{a}} = [2\mu_{\mathrm{m}}(Tt_{\mathrm{zm}} - Tt_{\mathrm{om}}) \cdot \exp(-\mu_{\mathrm{m}} \cdot \alpha_{\mathrm{m}}) + Tt_{\mathrm{om}}]^2$$

$$B_{\mathrm{a}} = v_{\mathrm{om}}$$

$$C_\mathrm{a} = 2Tt_\mathrm{zm}^2 \cdot D_\mathrm{m} \cdot \mu_\mathrm{m} \cdot \exp(-\mu_\mathrm{m} \cdot \alpha_\mathrm{m})[1 - \exp(-\mu_\mathrm{m} \cdot \alpha_\mathrm{m})]$$

$$E_\mathrm{a} = 2Tt_\mathrm{zm} \cdot Tt_\mathrm{om} \cdot D_\mathrm{m} \cdot \exp(-\mu_\mathrm{m} \cdot \alpha_\mathrm{m}) \cdot \{(Tt_\mathrm{zm} - Tt_\mathrm{om}) \cdot [1 - \mu_\mathrm{m}\alpha_\mathrm{m} - \exp(-\mu_\mathrm{m} \cdot \alpha_\mathrm{m})] - Tt_\mathrm{om} \cdot \alpha_\mathrm{m}/2\}$$

The correlated *phase frequency responses* for the disturbance $\widetilde{\Delta v_\mathrm{i}}$ are:

$$\varphi(f) = \text{arc tan}\left[-\frac{2\pi f \cdot C_\mathrm{a}}{A_\mathrm{a} \cdot B_\mathrm{a}}\right] \tag{5.25}$$

and for the disturbance $\widetilde{\Delta\mu}$:

$$\varphi(f) = \text{arc tan}\left[\frac{A_\mathrm{a} \cdot B_\mathrm{a}}{2\pi f \cdot C_\mathrm{a}}\right] \tag{5.26}$$

By means of Eqs.+5.25, 5.26 and 2.50 it is possible to give the delay thread lines L_dv (for a velocity disturbance Δv_i) or $L_{\mathrm{d}\mu}$ (for a friction coefficient disturbance $\Delta\mu$) as a quantity for the thread length which passes the transport system between the cause imprinting and the effect reaction of periodic disturbances. Considering Eq. 5.22 it is also possible to give here a result presentation versus the disturbance wavelength λ_f which is free of the output velocity v_om.

Before a quantitative analysis can be done it is necessary to calculate the sizes v_im, v_zm, Tt_im and Tt_om from the given sizes v_om and Tt_zm. If a preelongation of 0.3% is assumed in the input thread then $Tt_\mathrm{im} = Tt_\mathrm{zm}/1.003$ follows according to the continuity equation. Equation 5.10 was valid between input and output fineness of the thread along the friction line. With this it is also possible to calculate the velocities v_im and v_zm if the continuity equation $Tt_\mathrm{im} \cdot v_\mathrm{im} = \text{const.}$ is considered additionally.

Equations 5.23 to 5.26 have been analysed for the following combinations of process and product variables:

Tt_zm	= 3.4 tex
α_m	= $\pi/2$ (1/4 wrap)
	= 2π (1 wrap)
Tt_im	= 3.3898 tex
Tt_om	= 3.384 tex (for $\alpha_\mathrm{m} = \pi/2$)
	= 3.334 tex (for $\alpha_\mathrm{m} = 2\pi$)
v_om	= 100 m/min, 500 m/min, 1000 m/min
$v_\mathrm{zm}(\alpha = \pi/2)$	= 99.54 m/min, 497.76 m/min, 995.72 m/min
$v_\mathrm{zm}(\alpha = 2\pi)$	= 98.10 m/min, 490.41 m/min, 980.82 m/min
$v_\mathrm{im}(\alpha = \pi/2)$	= 99.84 m/min, 499.26 m/min, 998.52 m/min
$v_\mathrm{im}(\alpha = 2\pi)$	= 98.40 m/min, 491.94 m/min, 983.82 m/min
D_m	= 2 mm, 5 mm
μ_m	= 0.3

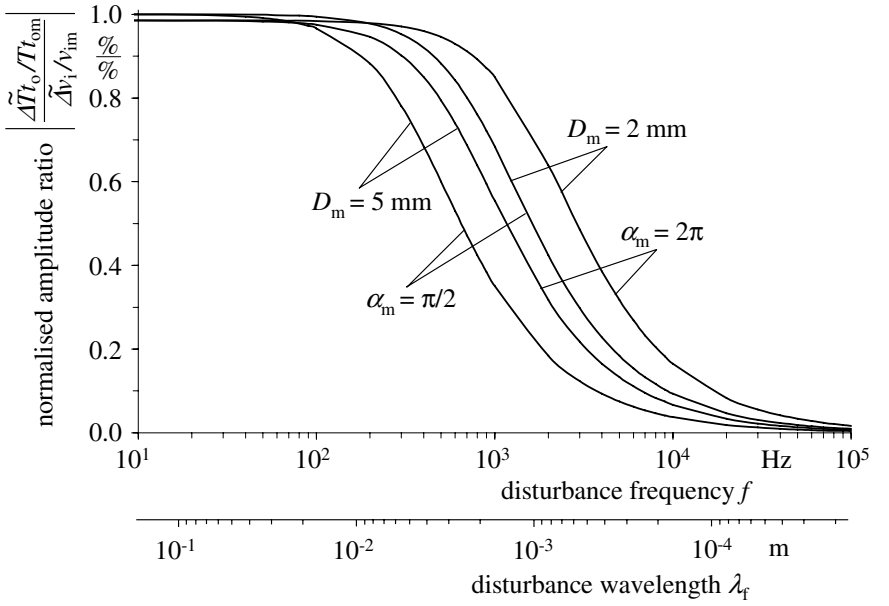

Fig. 5.8. Normalised amplitude frequency responses of fineness changes $\widetilde{\Delta T t_o}$ caused by input velocity changes $\widetilde{\Delta v_i}$ of a friction thread line after Fig. 5.3, output velocity $v_{om} = 100$ m/min

The results of the quantitative calculations are partly shown (for $v_{om} = 100$ m/min only) in Figs. 5.8 to 5.11. The following statements are also to be derived concerning the not presented results of the higher thread velocities:

a) $\widetilde{\Delta T t_o}$ will be smaller so the disturbance frequency f will be greater if a disturbance $\widetilde{\Delta v_i}$ effects. The reason for this is the dampening effect of the friction thread guide line (Fig. 5.8). This dampening effect starts at smaller frequencies the thicker the friction thread guide and the smaller the wrap angles are. It does not occur unless the disturbed thread lengths (disturbance wavelengths λ_f) are smaller than the wrap line on the thread guide.

b) A practically complete dampening of an input velocity disturbance occurs only at disturbance wavelengths in the thread of $\lambda_f < 0.15$ mm (according to influence times of the disturbance of < 0.1 ms!). Because all dynamic disturbances have as a rule a much longer influence time it is to be stated that all Δv_i disturbances at the input of a friction thread line will be transmitted greatly proportionally in the same $\Delta T t_o$ changes at the output (under the most suitable conditions of a constant output thread velocity).

c) The friction thread line effects (only for high frequency disturbances) a better disturbance decrease the greater its diameter and the smaller its

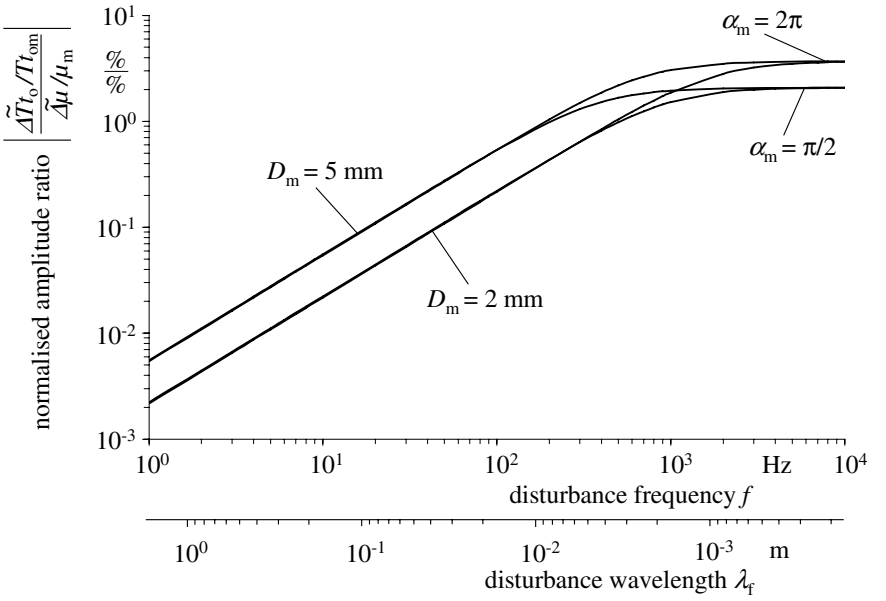

Fig. 5.9. Normalised amplitude frequency responses of fineness changes $\widetilde{\Delta Tt_o}$ caused by friction coefficient changes $\widetilde{\Delta\mu}$ of a friction thread line after Fig. 5.3, output velocity $v_{om} = 100$ m/min

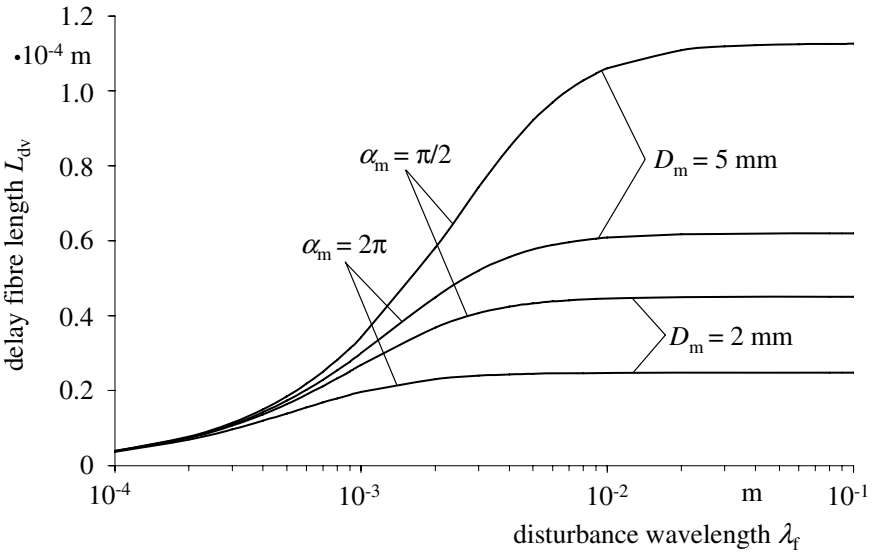

Fig. 5.10. Delay fibre length L_{dv} of a friction thread line after Fig. 5.3

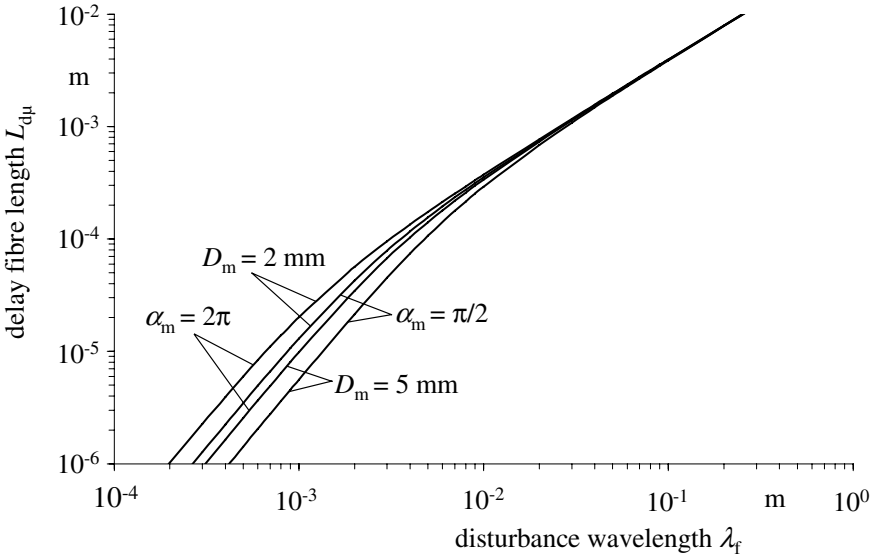

Fig. 5.11. Delay fibre length $L_{d\mu}$ of a friction thread line after Fig. 5.3

wrap angle is. This result suggests the following recommendation: To the realisation of an appointed mean thread tensile force at the input of a processing machine it is better to arrange serially several friction lines with large diameters and in each case small thread wrap angles (for instance a lattice brake) than only one friction thread line with a small diameter and a great wrap angle. If the use of only one friction thread line is possible then a great diameter is in its turn more favourable than a smaller on the same wrap angle.

d) The effect of friction coefficient changes or oscillations $\widetilde{\Delta\mu}$ to the fineness Tt_o are shown in Fig. 5.9. The relationships are valid for the case that the thread which runs into the friction thread line is braked with a constant brake force and it is constantly elongated (here 0.3%). Further it should be as valid as before: $v_o = v_{om} = \text{const}$.
Disturbances with a frequency of < 1 Hz (consequently all quasi steady state changes of the friction coefficient too) will not be of influence on the fineness. The fineness changes reach only less than 0.01% in this range for instance if the friction coefficient changes by 1%. The effect of the disturbances with the same dimensions is here (in opposite to the case of a input velocity disturbance discussed before) the greater in the rest of the frequency range the thicker the friction thread guide and the greater the thread wrap angle are. The amplitude frequency response of the model variants approximated before always to zero for high disturbance frequencies. In the present case of a friction coefficient disturbance the amplitude frequency response reaches a constant value (dependent on the thread line velocity; Fig. 5.9 only shows the

output velocity $v_{\mathrm{om}} = 100$ m/min) for disturbance frequencies of $> 5 \cdot 10^3$ to $> 5 \cdot 10^4$ Hz. It is the question here of a differential action which follows from the amplitude frequency response (5.24). Friction coefficient changes of 1% effect in this range even 2% (for $\alpha = \pi/2$) to 3% (for $\alpha = 2\pi$) fineness changes. However, this range is not effective because the according disturbance wavelengths in the thread are < 1 mm, that means below the length of the wrap or friction line. This amounts to, for the selected model relations, between 1.6 mm (for $D_{\mathrm{m}} = 2$ mm and $\alpha = \pi/2$) and 15.7 mm (for $D_{\mathrm{m}} = 5$ mm and $\alpha = 2\pi$). A disturbance dampening occurs for such short disturbance wavelengths because a mean value of the friction coefficient can only effect along a thread part which just passes the friction line.

e) The delay thread line L_{dv} always amounts to < 0.12 mm in the entire interesting disturbance wavelength range > 1 mm (Fig. 5.10). These only insignificant delays (compared to the disturbance wavelengths) are of completely no account for dynamic measurements of threads which are running about fixed friction elements due to their smallness.

f) The relations are similar for disturbances of the friction coefficient (Fig. 5.11). The amplitude frequency response (see Fig. 5.9) is so small for disturbance wavelengths > 10 cm (the delay thread length $L_{\mathrm{d}\mu}$ could amount here to more than 1 to 3 cm) that a nearly complete disturbance dampening exists. The delay thread lengths $L_{\mathrm{d}\mu}$ are already insignificantly small again (< 0.3 mm) at disturbance wavelengths below 2 to 3 mm if the amplitude frequency response reaches its full value.

Possibilities to the Dampening of Tensile Force and Tensile Elongation Variations in Thread Input Lines

In Sect. 5.1.5 it has been hinted that a skillful designing of delay lines can effect dampening to input velocity disturbances and their effects to fineness unevennesses. Such delay lines are found in many machines of thread or fibre processing. The thread is unwound normally from fixed or rotating supported, but not actively driven, supply bobbins by means of the machine taking-in elements. The so-called axial "over end unwinding" is predominant here. But, the radial thread unwinding from rotating supported supply bobbins can also be found. Numerous examples can be given as to the spinning, drawing, twisting, winding, texturing, warping, sectional warping, and knitting. Such thread input lines (Fig. 5.12) are more or less significant (according to process step and material kind) under the view point of the cause research to process disturbances or thread and fabrics unevennesses. The reason for this is that each uncontrolled thread input (which is realised in the described manner) is connected to thread tensile force and thread elongation changes.

Such changes can be the cause for changes of appointed textile-physical quality characteristics of the thread which will only be formed in the following process steps or will be optically visible displaced to the fabric possibly. But, they can "only" be responsible for an increased thread break frequency. In the following, possibilities and their efficiency to an effective dampening of thread tensile force and thread elongation changes without the use of special devices (for instance automatic controlled thread brakes) in connection with [296] and [297] will be discussed. These investigations are independent of the causing factors for such thread tensile force and thread elongation changes for instance hooked and plastered up threads on the supply bobbins, periodic changes of the unwinding geometry at threads which are unwinded radially from rotating supported supply bobbins.

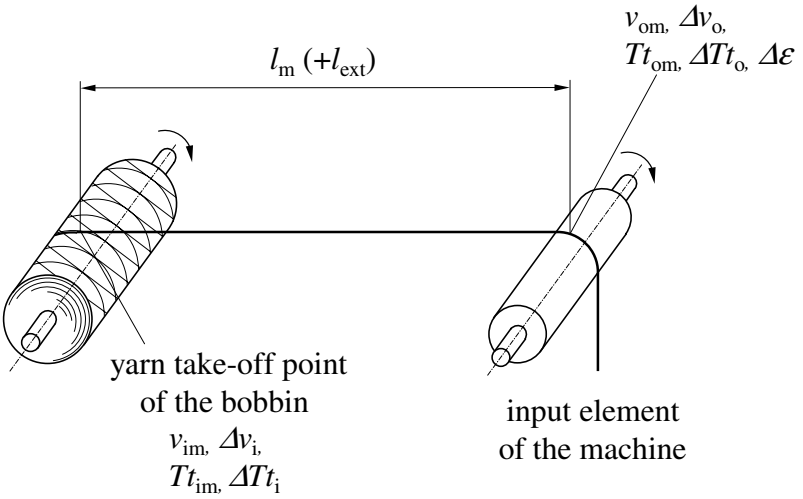

Fig. 5.12. Technological scheme of a thread input line

Input velocity changes Δv_i according to Fig. 5.12 are the most frequent cause for fineness changes ΔTt_o (and by this elongation and force changes $\Delta\varepsilon$ and ΔF, as will be demonstrated later in Sect. 6.2). Therefore the starting point of our views is the known *dynamic transfer function* of a delay line, which is derived from DEq. 5.1:

$$G(p) = \frac{\Delta Tt_o}{\Delta v_i} = \frac{Tt_{om}}{v_{im}} \cdot \frac{1}{1 + p \cdot \dfrac{l_m}{v_{om}}} \tag{5.27}$$

The elongation ε of a thread with the fineness Tt_i in the unloaded state and the fineness Tt_o in the elongated state is

$$\varepsilon = \frac{Tt_i}{Tt_o} - 1 \tag{5.28}$$

The partial differentiation of Eq. 5.28 to the three variables, which can be changeable, results in

$$\Delta\varepsilon = \frac{1}{Tt_{\mathrm{o}}} \cdot \Delta Tt_{\mathrm{i}} - \frac{Tt_{\mathrm{im}}}{Tt_{\mathrm{om}}^2} \cdot \Delta Tt_{\mathrm{o}} \tag{5.29}$$

We will not consider fineness changes of the input thread Tt_{i} in the present case ($\Delta Tt_{\mathrm{i}} = 0$). Equation 5.29 is simplified then to

$$\Delta\varepsilon = -\frac{Tt_{\mathrm{im}}}{Tt_{\mathrm{om}}^2} \cdot \Delta Tt_{\mathrm{o}} \tag{5.30}$$

ΔTt_{o} from Eq. 5.30 introduced into Eq. 5.27 results to the *amplitude frequency response*

$$|G(\mathrm{j}f)| = \left| \frac{\widetilde{\Delta\varepsilon}}{\widetilde{\Delta v_{\mathrm{i}}}/v_{\mathrm{im}}} \right| = (-)\frac{Tt_{\mathrm{im}}}{Tt_{\mathrm{om}}} \left[1 + \left(\frac{2\pi f \cdot l_{\mathrm{m}}}{v_{\mathrm{om}}} \right)^2 \right]^{-1/2} \tag{5.31}$$

The amplitude frequency response of Eq. 5.31 is shown versus the length of the input line l_{m} for different frequencies of the disturbance $\widetilde{v_{\mathrm{i}}}$ in Fig. 5.13. The diagram is related to an experimental investigation of a twister. The velocity v_{om} amounted to 58 m/min.

Thread input velocity oscillations $\widetilde{\Delta v_{\mathrm{i}}}$ should only effect small $\widetilde{\Delta\varepsilon}$ oscillations in a stable process. That means, the amplitude frequency response should be as small as possible or even zero. A relatively simple technological-constructive method insists on the extension of the thread input (delay) line as long as possible (compare Fig. 5.13). A further modified quantitative analysis of the solution equation for the dynamic mathematical model can be given as follows.

Dependent on

- the length l_{m} of any existing thread input line on a machine,
- the thread transport velocity v_{om},
- the frequency f of the thread tensile force and the thread elongation changes

an exactly quantitative predetermined extension of the input line l_{ext} can be calculated, in which the existing amplitudes of the thread tensile force and thread elongation oscillations are reduced by a wished reduction factor R. This reduction factor R is defined as

$$R = 1 - \frac{|G(\mathrm{j}f)| \quad (\text{input line } (l_{\mathrm{m}} + l_{\mathrm{ext}}))}{|G(\mathrm{j}f)| \quad (\text{input line } l_{\mathrm{m}})} \tag{5.32}$$

Equation 5.32 inserted into Eq. 5.31 yields:

$$R = 1 - \sqrt{\frac{1 + \left(\dfrac{2\pi f \cdot l_{\mathrm{m}}}{v_{\mathrm{om}}} \right)^2}{1 + \left[\dfrac{2\pi f \cdot (l_{\mathrm{m}} + l_{\mathrm{ext}})}{v_{\mathrm{om}}} \right]^2}} \tag{5.33}$$

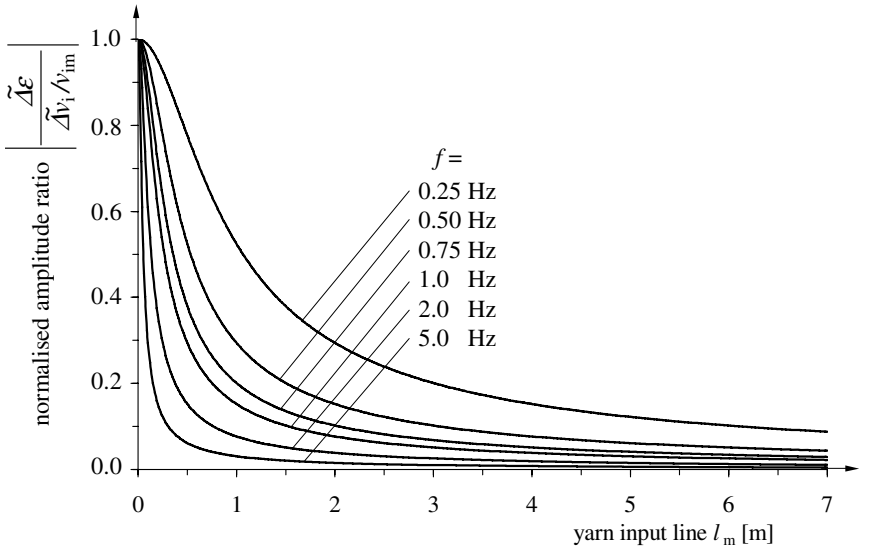

Fig. 5.13. Normalised amplitude transfer coefficients for changes of thread elongations $\widetilde{\Delta\varepsilon}$ caused by changes of the thread input velocity $\widetilde{\Delta v_i}$ of a thread input line

Equation 5.33 dissolved to l_{ext} results in the condition for the necessary extension of the thread input line at the wished reduction factor R

$$l_{ext} = \frac{\sqrt{R \cdot v_{om}^2 \cdot (2 - R) + (120\pi \cdot f \cdot l_m)^2}}{120\pi \cdot f \cdot (1 - R)} - l_m \tag{5.34}$$

The following dimensions are used:

l_m, l_{ext}	m
v_{om}	m/min
f	Hz
R	dimensionless, possible range from 0 (no reduction of disturbances) until 1 (full dampening of disturbances)

The necessary input line extension l_{ext} can also be appointed by means of a simplified approximation relation 5.35 (the basis for this is also Eq. 5.34), if a reduction of the thread tensile force and thread elongation changes have reached the half according to those by an unextended input line (reduction factor $R = 0.5$). This is much better to handle, but it requires somewhat greater l_{ext}-values for high thread line velocities ($v_{om} > 500$ m/min) and simultaneously small disturbance frequencies ($f < 5$ Hz). These l_{ext}-values are concerning the desired effect.

$$l_{ext} \approx 15 \cdot v_{om}/f + l_m \quad \text{(valid for } R{=}0.5) \tag{5.35}$$

The following dimensions are used:

l_m, l_ext	m
v_om	m/s
f	min^{-1}

Quantitative data to the choice of input line extensions under concrete technological conditions can be taken away in Fig. 5.14.

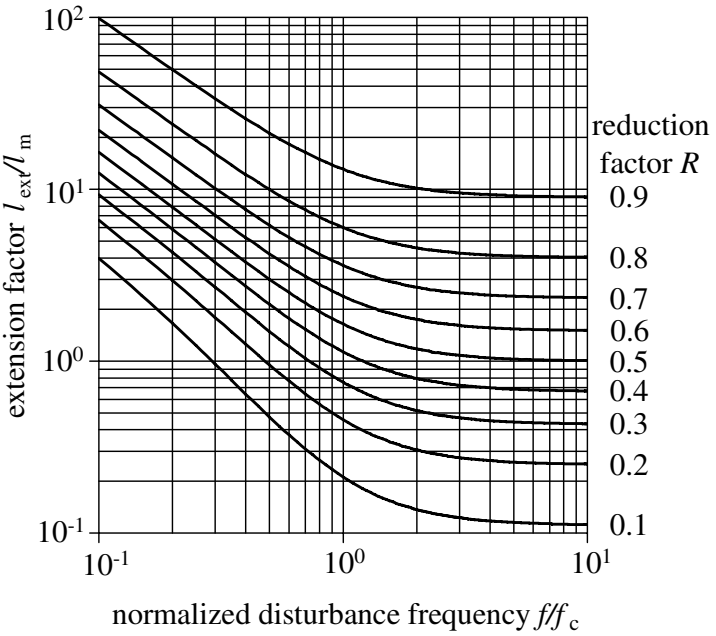

Fig. 5.14. Necessary extension factor $l_\mathrm{ext}/l_\mathrm{m}$ dependent upon the disturbance frequency ratio f/f_c and on the reduction factor R

The use is the following:
One appoints the critical frequency f_c of the input line by means of Eq. 2.49 or Fig. 4.7 on the basis of the already present input line length l_m and winding up thread or input velocity into the machine v_om. It is also possible to find out the extension factor $l_\mathrm{ext}/l_\mathrm{m}$ according to the already present input line l_m, which is to be realised for a dampening of the changes with the appointed reduction factor R.
If the necessary input line extension cannot be realised in a straight line on the machine then the whole length can be realised by means of thread deflection elements. However, the latter must be thread guide elements with light running rolls to reach the full dampening effect [297].

The efficiency of an input line extension (calculated on the basis of the developed theoretical fundamentals) should be demonstrated finally using variation coefficients derived from the experimentally measured thread tensile force time functions in the input line of a ring twister (Fig. 5.15).
The normal input line amounted to $l_{\mathrm{m}} = 0.42$ m, and the thread input ve-

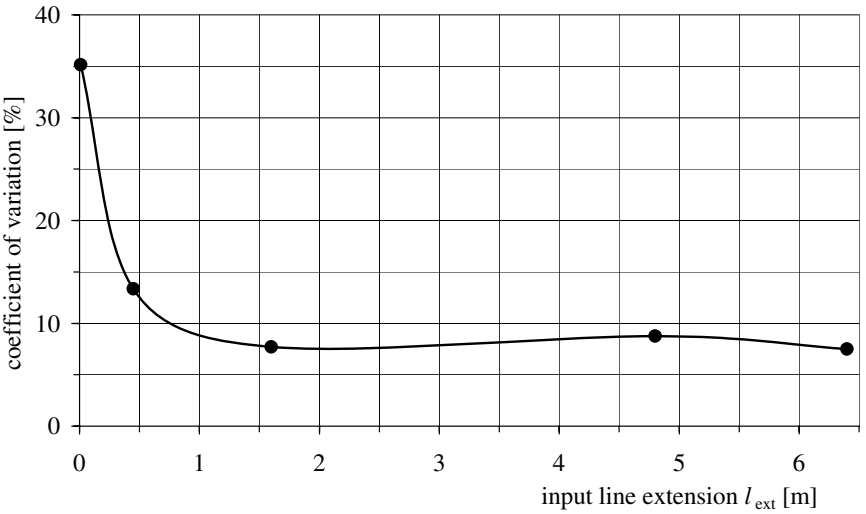

Fig. 5.15. Variation coefficients of tensile force time functions on a *Mouliné*-twister for different input line extensions l_{ext}, fibre material: PET 11 tex (20), texturised, $v_{\mathrm{om}} = 58$ m/min

locity to $v_{\mathrm{om}} = 58$ m/min ($f_{\mathrm{c}} = 0.37$ Hz). It was to observed through this condition that a main frequency of the thread tensile force changes (and with this also of the thread elongation) of 0.75 Hz caused by a radially unround thread backing-off from a rotating supported supply bobbin. The tensile force changes amount nevertheless to $\pm 50\%$ around the mean value of 75 mN and result in a variation coefficient of 35.15% ($l_{\mathrm{ext}} = 0$). These led to the induced elongation changes of the same relative quantity to distinct shade disturbances of the manufactured plied threads which consisted of two such supply threads of different fundamental colours. Input line extensions of $l_{\mathrm{ext}} = 0.45$ m led to a variation coefficient of 13.34% and the disturbed quality deficiencies were removed at the input line extensions $l_{\mathrm{ext}} \geq 1.6$ m. The variation coefficients of the tensile force time functions decrease then to $< 9\%$ (see also Sect. 6.4.2 and Fig. 5.15 again).
This technological example shows that an undisturbed thread run can be realised throughout without greater additional expense, if the dynamic transmission regularities are strictly used.

Fibre Influence by Means of Dynamics of Thread Traverse Motion at Winders

A further interesting application of the dynamic model of a delay thread line (applied to a concrete technological situation) is the analysis of the fineness influence caused by the periodic thread traverse motion at the winders. The characteristics of the appropriate extensive investigations [298] and some results are presented as follows. First, a few remarks to the motive of such investigations:

a) The traverse motion system permanently imprints the thread periodic property changes along its length axis which can be recorded as elongation and fineness changes. Such changes can evoke considerable molecular structure changes of the threads, particularly at the spinning machines for man-made fibres, because these changes are imprinted during the decisive phase of the structure development [299].

b) Already periodic elongation and fineness changes of 1% (!) can be the cause for visible dyeing defects in special products of man-made fibres [300].

c) A well-defined relationship exists between the quantity of the thread breaks at special processing processes and the fineness fluctuation amplitudes imprinted by the thread traverse motion process at the man-made fibre spinning machine.

d) Elongation and thread tensile force fluctuations caused by the traverse motion can involve deviations of the reel body from the desired cylindrical shape which leads to local different mill work particularly at the friction roll drives as a consequence of different contact pressures.

The thread line between the delivery godet and the wind-up bobbin can be taken in as a delay thread line (Fig. 5.16) which also includes the common case of an asymmetric traverse motion triangle (Fig. 5.17).

The basis for the derivation of the dynamic model is therefore the common linearised DEq. for a delay line. The cause variable of the fineness disturbances $\Delta T t_{\mathrm{o}}$ of the winded thread are the periodically enforced changes of the length Δl of the delay line. The short friction lines on the thread guides at the top of the traverse motion triangle and of the traverse motion are itself neglected in the following. The dynamic model DEq. derives from Eq. 4.7 and is changed to:

$$(v_{\mathrm{om}} + p \cdot l_{\mathrm{m}}) \cdot \Delta T t_{\mathrm{o}} + p \cdot T t_{\mathrm{om}} \cdot \Delta l = 0 \tag{5.36}$$

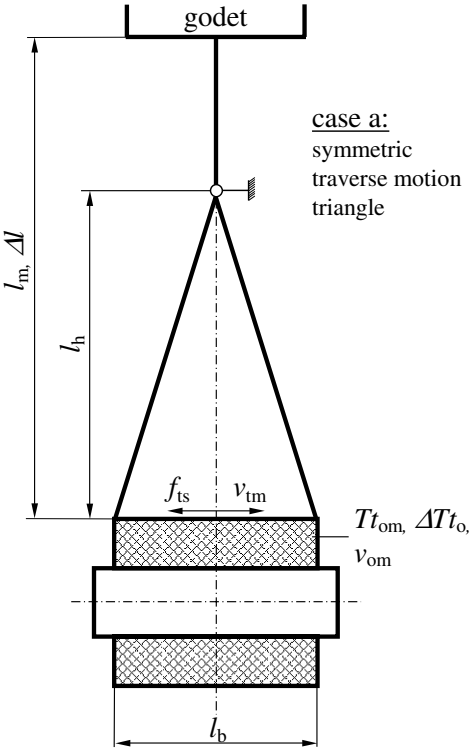

Fig. 5.16. Technological scheme of the thread traverse motion, case a

The symbols in Figs. 5.16, 5.17 and Eq. 5.36 mean:

Tt_{om}	mean value of the fineness of thread at the bobbin wind-up point approaching from the traverse motion triangle
l_m	mean value of the thread length between godet and wind-up point of the bobbin
v_{om}	mean value of the velocity of thread which the bobbin winds up (output or wind-up velocity)
l_h	height of the traverse motion triangle
v_{tm}	mean value of the linear velocity of traverse motion thread guide
l_b	length of the bobbin
f_{ts}	frequency of the traverse motion thread guide for the operation of one twice stroke, that means its motion from the left bobbin edge to the right and back
e	asymmetry parameter
p	differential operator d/dt

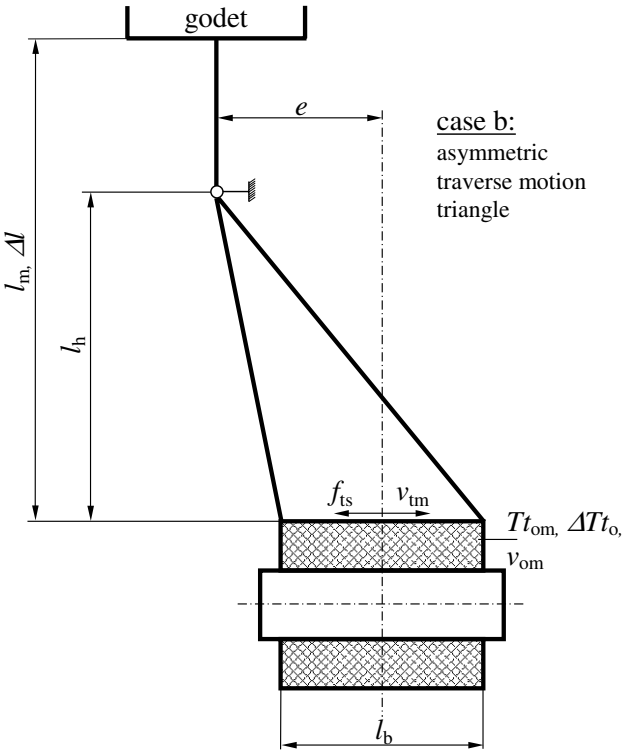

Fig. 5.17. Technological scheme of the thread traverse motion, case b

The resolution of the DEq. 5.36 for impulse-like Δl-disturbances (it is equivalent to the first derivation of the step response Eq. 4.36) is

$$\Delta T t_o \perp \Delta l = \Delta l \cdot \frac{T t_{om} \cdot v_{om}}{l_m^2} \cdot \exp\left(-\frac{v_{om}}{l_m} \cdot t\right) \tag{5.37}$$

If the change Δl caused by the traverse motion is impulse-like then the effected fineness change can already be calculated by means of Eq. 5.37. However, the time function of the change Δl is to be derived from the root laws of the rectangular triangle (see Figs. 5.16, 5.17). This can be derived after several intermediate steps (not further described here) and simplifications:
Forward motion (thread guide goes from the left bobbin edge to the right with the linear velocity $v_{tm} = 2 \cdot l_b \cdot f_{ts}$)

$$\Delta l(t) = A_b \cdot t^2 + B_b \cdot t \tag{5.38}$$

Backward motion (thread guide goes from the right bobbin edge to the left with the linear velocity $v_{tm} = 2 \cdot l_b \cdot f_{ts}$)

$$\Delta l(t) = A_b \cdot t^2 + C_b \cdot t \tag{5.39}$$

The abbreviations $A_\mathrm{b}, B_\mathrm{b}$ and C_b mean:

$$A_\mathrm{b} = 8f_\mathrm{ts}^2 \cdot \left[\sqrt{l_\mathrm{h}^2 + (e + 0.5 \cdot l_\mathrm{b})^2} + \sqrt{l_\mathrm{h}^2 + (e - 0.5 \cdot l_\mathrm{b})^2} - 2\sqrt{l_\mathrm{h}^2 + e^2}\right]$$

$$B_\mathrm{b} = 2f_\mathrm{ts} \cdot \left[4\sqrt{l_\mathrm{h}^2 + e^2} - 3\sqrt{l_\mathrm{h}^2 + (e - 0.5 \cdot l_\mathrm{b})^2} - \sqrt{l_\mathrm{h}^2 + (e + 0.5 \cdot l_\mathrm{b})^2}\right]$$

$$C_\mathrm{b} = 2f_\mathrm{ts} \cdot \left[4\sqrt{l_\mathrm{h}^2 + e^2} - 3\sqrt{l_\mathrm{h}^2 + (e + 0.5 \cdot l_\mathrm{b})^2} - \sqrt{l_\mathrm{h}^2 + (e - 0.5 \cdot l_\mathrm{b})^2}\right]$$

Figure 5.18 shows the resulting percent thread length shifts in the traverse motion triangle versus the bobbin length axis for different geometrical conditions.

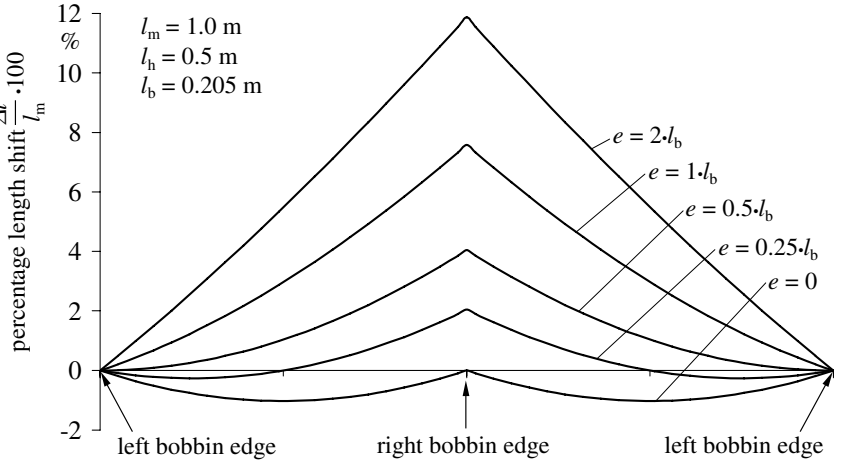

Fig. 5.18. Per cent thread length shifts in the traverse motion triangle caused by the traverse motion

In the next step, the resolution of the DEq. 5.36 for the time courses of the disturbances Δl defined by Eqs. 5.38 and 5.39 has to be found. The LAPLACE-transformation makes a resolution algorithm available for any time course by means of the convolution integral (see for instance [13]). The integral applied to the present case can be read as:

$$\underline{\Delta T t_\mathrm{o}}/\overline{\Delta l} = \int_0^t \Delta l(\tau) \cdot \frac{T t_\mathrm{om} \cdot v_\mathrm{om}}{l_\mathrm{m}^2} \cdot \exp\left(-\frac{t - \tau}{l} \cdot v_\mathrm{om}\right) d\tau \qquad (5.40)$$

The integrand consists of the product of the disturbance time function (here $\Delta l(\tau)$, the time variable t is to be substituted by the integration variable τ – Eqs. 5.38 and 5.39 are to be inserted practically) and the impulse response function of the wanted goal variable (here $\Delta T t_\mathrm{o}$) for the same cause variable

(here Δl, that means Eq. 5.37). The time variable is to be substituted finally by shifting the term $t - \tau$.
After the integrations, one gets the following related time functions of the percent fineness changes caused by the traverse motion thread guide:
Forward motion

$$\frac{\Delta T t_{\mathrm{o}}}{T t_{\mathrm{om}}} = \frac{100}{v_{\mathrm{om}}} \left\langle \left(\frac{2A_{\mathrm{b}} \cdot l_{\mathrm{m}}}{v_{\mathrm{om}}} - B_{\mathrm{b}} \right) \left[1 - \exp\left(-\frac{v_{\mathrm{om}}}{l_{\mathrm{m}}} \cdot t \right) \right] - 2A_{\mathrm{b}} \cdot t \right\rangle \quad (5.41)$$

Backward motion

$$\frac{\Delta T t_{\mathrm{o}}}{T t_{\mathrm{om}}} = \frac{100}{v_{\mathrm{om}}} \left\langle \left(\frac{2A_{\mathrm{b}} \cdot l_{\mathrm{m}}}{v_{\mathrm{om}}} - C_{\mathrm{b}} \right) \left[1 - \exp\left(-\frac{v_{\mathrm{om}}}{l_{\mathrm{m}}} \cdot t \right) \right] - 2A_{\mathrm{b}} \cdot t \right\rangle \quad (5.42)$$

The mathematical basis is now given for quantitative investigations by means of Eqs. 5.41 and 5.42. The changes $\Delta T t_{\mathrm{o}}$ are completely calculable only for a single stroke of the traverse motion thread guide, because the time functions $\Delta l(t)$ are also not informable close too (the derivations are not defined at the turning back points of the bobbin edges and should be taken from one equation to the other). The destination of the steady state oscillation state is only possible by repeatedly modified joinings of Eqs. 5.41 and 5.42. It should be observed when the change time functions of two successive double strokes of the traverse motion thread guide do not distinguish themselves. It is also only possible to calculate the steady state oscillation state iteratively as a sequence of mathematical completely calculable single time courses of the thread fineness changes which partly depend on each other. Closed resolutions have become known (these develop the periodic, not continuous $\Delta l(t)$-course into a *Fourier*-row and only use the first element for further calculations [299]), but only with greater mistakes at the turning back points. However, the $\Delta l(t)$-course possesses the greatest gradation at only this points.

Extensive quantitative investigations have been carried out which included variations of the wind-up velocity v_{om} (1000...6000 m/min), the height of the traverse motion triangle l_{h} (0.3...1 m), the length of the bobbin l_{b} (0.135...0.205 m), the twice stroke frequency of the traverse motion thread guide f_{ts} (500...1500 min^{-1}), and the asymmetry of the top of the traverse motion triangle e $(0...2 \cdot l_{\mathrm{b}})$. Some selected result diagrams are shown in Figs. 5.19 (transient oscillations of the percent fineness shifts), 5.20 (percent maximal spans of the fineness shifts), and 5.21 (percent fineness shifts on the bobbin edges). The valid technological conditions should be learned from the signatures of the figures in each case.

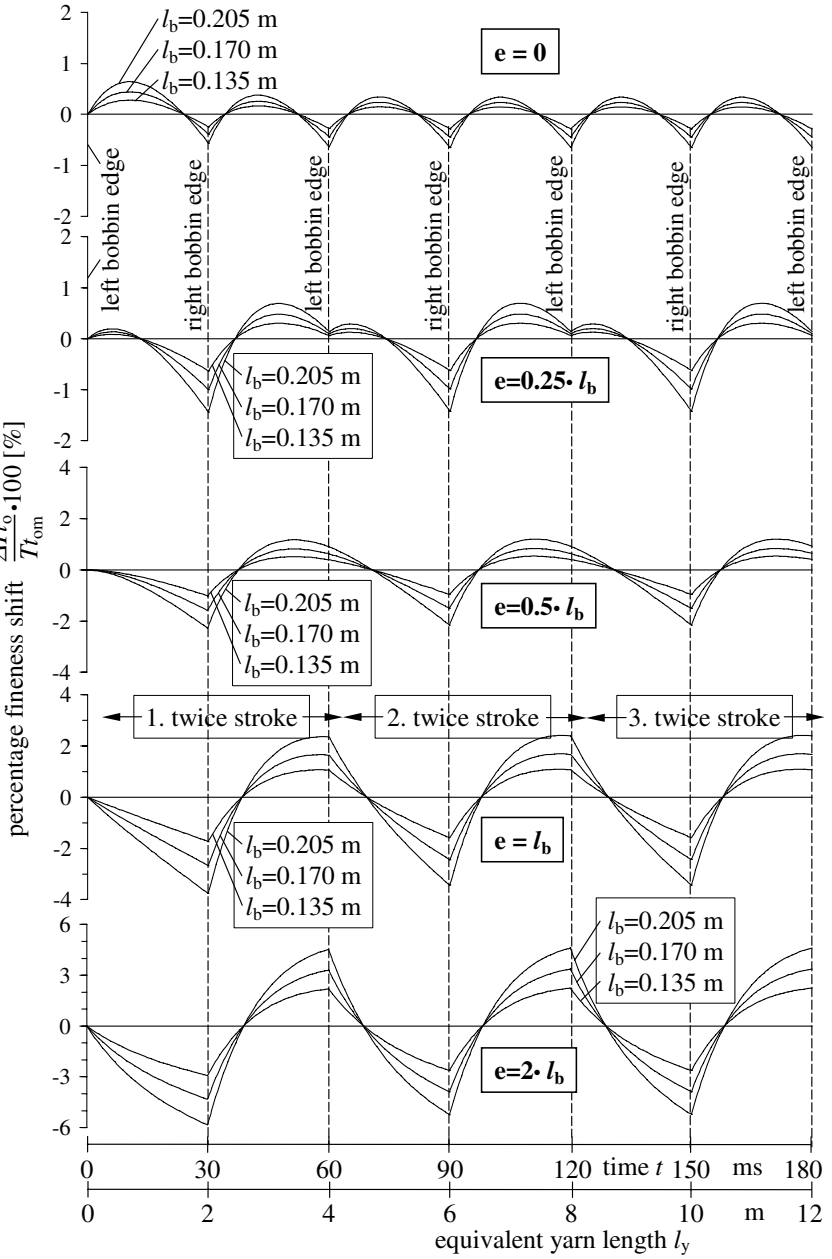

Fig. 5.19. Transient oscillations of percent fineness shift caused by the thread traverse motion; $l_m = 1.0$ m, $l_h = 0.5$ m, $v_{om} = 4000$ m/min, $f_{ts} = 1000$ min^{-1}

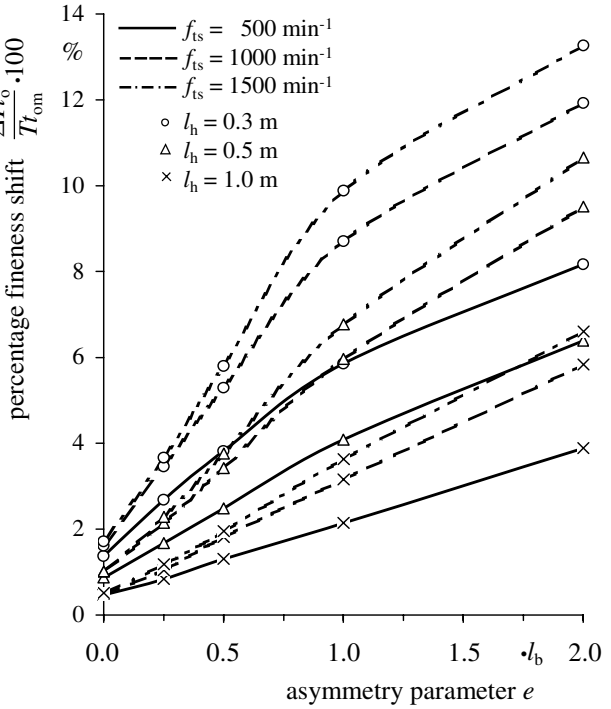

Fig. 5.20. Percent maximal span of the fineness shifts caused by the thread traverse motion; $l_m = 1.0$ m, $l_b = 0.205$ m, $v_{om} = 4000$ m/min

The following statements and conclusions can be given on the basis of all calculation results (also those which are not shown in the figures):

a) The fineness change course shows (for $< 0.5 \cdot l_b$) twice the frequency compared to systems with $> 0.5 \cdot l_b$ (see Fig. 5.19) at symmetric and little asymmetric traverse motion triangles.

b) The amplitudes of the shifts are smaller than $\pm 1\%$ for symmetric and slightly asymmetric traverse motion triangles and the so-called technological operating point ranges. They increase more for large asymmetries of the traverse motion triangle. If e increases from 0 to $0.5 \cdot l_b$ (triangle top is situated above the bobbin edge) then the fineness shift will nearly quadruple (see Fig. 5.20).

c) A strong ascent of the fineness shifts can be observed if the top of the traverse motion triangle moves nearer to the bobbin. The fineness shift is nearly doubled in the investigated operation range if l_h is halved (see Fig. 5.20).

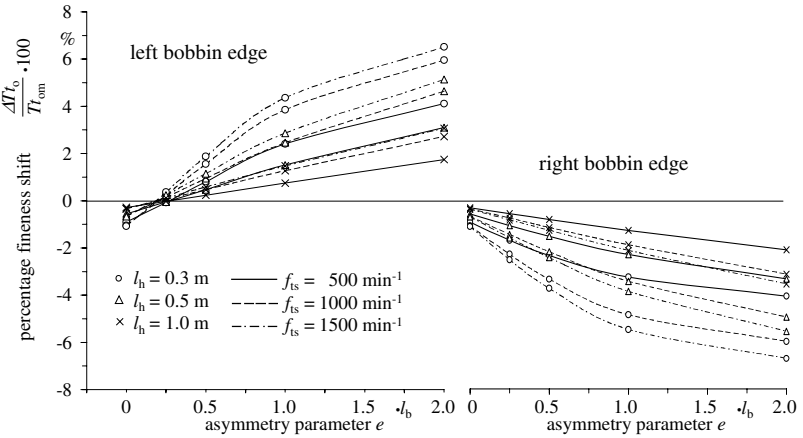

Fig. 5.21. Percent fineness shifts on the bobbin edges caused by the thread traverse motion; $l_m = 1.0$ m, $l_b = 0.205$ m, $v_{om} = 4000$ m/min

d) The fineness shifts also increase with longer bobbins (see Fig. 5.19).

e) High wind-up velocities dampen the fineness shifts. This is then the special case if they are connected with small double stroke frequencies of the traverse motion thread guide, because the thread will be transported faster out of the traverse motion field for these cases the fineness shift is then imprinted by the Δl-lengthening or -shortening.

f) The influence of the traverse motion frequency is quantitatively different. In principle high frequencies effect greater fineness shifts, but their influence is strongly dependent upon the selected wind-up velocity. The influence is weakly stamped for small wind-up velocities and strongly stamped for high wind-up velocities (see Fig. 5.20).

g) Symmetric traverse motion systems produce a symmetric bobbin structure in which fineness minima appear at the bobbin edges. These are double the size of the fineness maxima in the middle of the bobbin (not presented here). Bale-shaped bobbins with reduced bobbin edges will arise always with this (see Fig. 5.21).

h) Asymmetric traverse motion triangles produce in principle greater fineness shifts. But, the bobbin structure is also seemingly unsymmetric for such systems: The one bobbin edge will be built up stronger and corresponds to the mean value of the fineness, the other will then be provided with the maximum negative fineness shifts. It does not appear bale-shaped or barrel-shaped, but leads to conical bobbins (see Fig. 5.21).

i) The following constructive and technological conditions can be proposed which allow for the smallest fineness shifts (caused by the traverse motion):
- symmetric structure of the traverse motion system ($e = 0$)
- greatest possible height of the traverse motion triangle ($l_h > 0.5$ m)
- as short as possible bobbins (manifold wind-up technology is ideal if each single bobbin can get its own symmetric traverse motion triangle!)
- lowest possible traverse motion velocity, that means small double stroke frequency.

The fineness shifts or changes (caused by the traverse motion system) can be held constant under these conditions at smaller than $\pm 0.2\%$ without special resources (for instance stress compensation rolls).

5.2 Dynamics of the Twist Transfer at the False Twist Texturing

5.2.1 Task

The majority of the PET and PA fine yarns manufactured today is texturised. The preferred process is the false twist (or FT-) texturing which realises more than 90% of all texturised fine yarns.
A twisting element gives the yarn torsional twists which are strongly imprinted (fixed) on this by means of consecutive heating and cooling. The imprinted so-called false twists will be dissolved after passing the twisting element and the texturised (equipped with a strong fixed curling) yarn is wound up. One distinguishes the magnetic spindle and the friction disk principles according to the kind of twist generation by means of the different false twist spindles. Both principles should generate torsional, or false twists, to the yarn on an only limited, usually short distance of the yarn length axis by means of quickly rotating machine elements. The torsion twist is to be generated by an intensive, as slip poor, as possible friction transmission through the yarn surface. It is not the task of this section to discuss the different advantages and disadvantages of the different basic principles of the false twist texturing. A lot of special literature is available concerning this.
However, some dynamic cause-effect relations of this process should be explained which regard the effect or goal variable twist density T_D of the texturised yarn in the texturing and setting zone. The expert knows from a-priori knowledge (one should once again recall to Sect. 2.5.1 - proposed steps for the working out the dynamic model) that texturing mistakes (that means, changes of the curling intensity along the texturised yarn) are caused mainly by dynamic changes of the product variable twist density T_D which only exists during the running process.

It is therefore obvious to elaborate a dynamic model of this product variable which theoretically founds the relationship of the different process and product variables. This should help to clear up the process analytical relationships between the disturbances of the variable T_D and the product quality. In the past, investigations have been done for either the steady state process only or the experimental results of measured twist densities and (also partly) for their changes (see [301] until [310]).

Nevertheless, it is to be remarked that simplifications and approximations (more than in other sections of the book) have been necessary for the following demonstrated investigations because of the complicated structure of the exact physical-analytical relationships. This necessity aims at presenting explicit resolution equations which should be usable without any further special knowledge. This should allow for qualitatively correct tendency statements in their proportions between each other on the one hand, but on the other is only restricted quantitative exactness connected with this.

5.2.2 Mathematic-Dynamic Model

Differential Equation of the Twist Density and its Solutions

The development of the DEq. for the twist density of the yarn in the texturing and setting zone T_D enforces some previous considerations and results which were informed in Sect. 5.1 (as a-priori knowledges to be declared now). The earlier recommended registration and sorting of all process and product variables, which are involveded in the process and are probably connected with each other via cause-effect relations (see Sect. 2.5.1) should be carried out here only verbally. The basis is the Fig. 5.22 which shows the necessary process and product variables of the thread course of a false twist texturing process with magnetic spindle twist element(magnetic false twist spindle) in a strongly simplified form.

It is irrelevant, by the way, whether the twists are generated by a friction spindle element or by a magnetic spindle. One can imagine that the several, short in series operating twists transmitting yarn touch points of a friction spindle are collected only in one integral effectual point. This one point then carries out a sum of effectual friction on the yarn. An explanation of this will be given at the end of this section.

The twist density T_D, as the quantity of twists referred to the thread length, (measured in the twisted state) obviously depends on

- the speed of the false twist spindle n_s,
- the present velocity of the twisted thread in the texturing and setting zone v_i, and
- the thread fineness Tt.

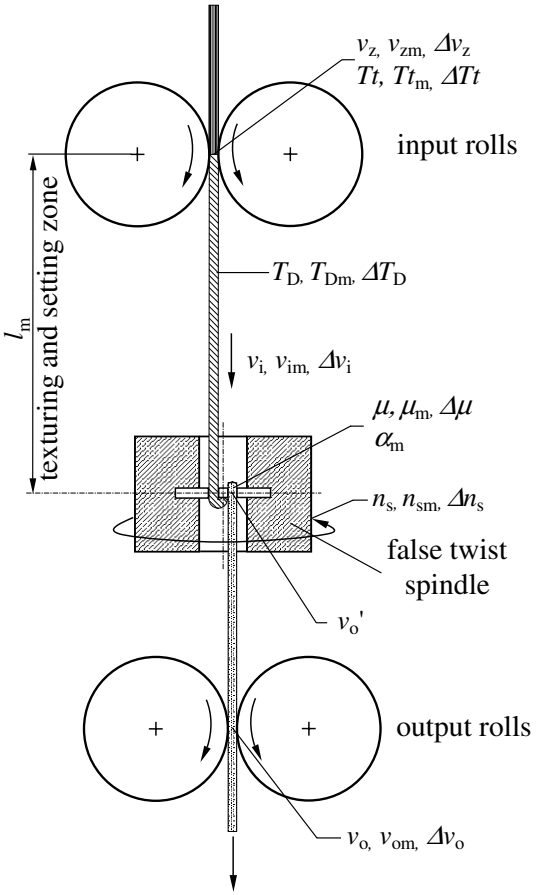

Fig. 5.22. Technological scheme of the false twist texturing process with magnetic twist spindle

The velocity of the twisted thread v_i (simultaneously equal to the input velocity of the twisted thread into the false twist spindle) finally turns up dependent upon

- the input velocity of the untwisted thread into the input rolls v_z,
- the thread output velocity v_o,
- the rope friction factor $e^{\mu\alpha_m}$,
- the thread fineness Tt, and
- the speed of the false twist spindle n_s.

Changes of the thermic process and product variables (for instance thread temperatures) and their effects on the thread properties (for instance changes of the E-moduli and the following changes of the thread tensile force rela-

tions before and after the twisting element) will be neglected, simultaneous to a draw texturing process which imprints the thread additionally a greater plastic longitudinal orientation elongation. Some explanatory remarks will be given to the latter at the end of this section.

If the texturing and setting zone l_m is taken as a store and exchange line of the yarn torsional twists per time unit, then the dynamic basic Eq. 2.23 (applied to the present case in a modified form) can be formulated as follows:

$$\frac{\text{twists inflow}}{\text{time}} = \frac{\text{twists discharge}}{\text{time}} + \frac{\text{changes of twists}}{\text{time}} \tag{5.43}$$

It is to be put in as:

twists inflow/time $= n_\mathrm{s}$ (where no slip is assumed at the twisting element)
twists discharge/time $= T_\mathrm{D} \cdot v_\mathrm{i}$
changes of twists/time $= \dot{T}_\mathrm{D} \cdot l_\mathrm{m}$
(in which the same mean value of the twist density is assumed through the whole line l_m)

The DEq. of the twist density can be written then as:

$$n_\mathrm{s} = T_\mathrm{D} \cdot v_\mathrm{i} + p \cdot T_\mathrm{D} \cdot l_\mathrm{m} \tag{5.44}$$

where $p = \dfrac{\mathrm{d}}{\mathrm{d}t}$ is the well-known LAPLACE-operator.
The steady state relation for the twist density $T_\mathrm{D} = n_\mathrm{s}/v_\mathrm{i}$ follows for $\dot{T}_\mathrm{D} = 0$ of course unrestricted.
Equation 5.44 contains the independent not-freely-adjustable process variable v_i which must be expressed by means of technological independent process and product variables. The shortening factor K_s which represents the ratio of the twisted length l_t to the stretched, untwisted length l_u of one twist of the same in each case unloaded yarn piece must first of all be defined:

$$K_\mathrm{s} = l_\mathrm{t}/l_\mathrm{u} \tag{5.45}$$

Obviously it is also valid:

$$K_\mathrm{s} = v_\mathrm{i}/v_\mathrm{z} \tag{5.46}$$

The thread length of one twist l_t is

$$l_\mathrm{t} = l_\mathrm{m}/z \tag{5.47}$$

where z is the number of the total twists in the zone l_m, that means:

$$z = \frac{n_\mathrm{s} \cdot l_\mathrm{m}}{v_\mathrm{i}}$$

consequently

$$l_{\mathrm{t}} = \frac{v_{\mathrm{i}}}{n_{\mathrm{s}}} = \frac{K_{\mathrm{s}} \cdot v_{\mathrm{z}}}{n_{\mathrm{s}}} \tag{5.48}$$

The stretched, untwisted length l_{u}, of the same yarn piece, is calculated from the periphery of the cross sectional area of the multifilament (twisted) yarn which we will formally introduce as $\pi \cdot D_{\mathrm{y}}$ (D_{y} is in this aspect the diameter of the multifilament (twisted) yarn).
The stretched, untwisted length of one yarn twist finally results as the length of the line of a screw with the diameter D_{y} and with the ascent height l_{u} to:

$$l_{\mathrm{u}} = \sqrt{(\pi \cdot D_{\mathrm{y}})^2 + \frac{v_{\mathrm{i}}^2}{n_{\mathrm{s}}^2}} \tag{5.49}$$

v_{i} is determined in the real process by v_{o} (caused by the output rolls) which effects the friction body of the twisting element into the process line l_{m}.

We assume that the yarn along the whole friction thread line will be twisted on the twisting element and the false twists will be immediately dissolved in turn, if the twisted yarn leaves the friction body down to the output. In this peel-off moment in the twisted state, the yarn should possess the velocity v'_{o} and, immediately afterwards (after dissolving of the twists), the output velocity v_{o}. This is valid as:

$$v_{\mathrm{o}} = \frac{v'_{\mathrm{o}}}{K_{\mathrm{s}}} \tag{5.50}$$

The already deviated relationships of the thread transport along a friction thread line (see Sect. 5.1.4) must be validated to the estimation of the velocity transition from v_{i} to v'_{o}. The desired relation can be derived from Eq. 5.10 considering the continuity equation of a transported yarn without losses $Tt_{\mathrm{i}} \cdot v_{\mathrm{i}} = \mathrm{const}$. It is read as, using the symbols of our problem:

$$\frac{v'_{\mathrm{o}}}{v'_{\mathrm{z}}} = \left(\frac{v_{\mathrm{i}}}{v'_{\mathrm{z}}} - 1\right) \cdot \exp(\mu \cdot \alpha_{\mathrm{m}}) + 1 \tag{5.51}$$

The independent given yarn input velocity v_{i} is to be inserted into Eq. 5.51 in its reduced form

$$v'_{\mathrm{z}} = v_{\mathrm{z}} \cdot \ K_{\mathrm{s}} \tag{5.52}$$

because the twisted yarn is this aspect on the friction body.
Finally v_{i} is to be now written by using the Eqs. 5.45 and 5.48 to 5.52

$$v_{\mathrm{i}} = \sqrt{[(v_{\mathrm{o}} - v_{\mathrm{z}}) \cdot \exp(-\mu\alpha_{\mathrm{m}}) + v_{\mathrm{z}}]^2 - (\pi \cdot D_{\mathrm{y}} \cdot n_{\mathrm{s}})^2} \tag{5.53}$$

Before the final DEq. of the twist density T_D will be formulated, the yarn diameter D_y shall be expressed depending on the yarn fineness Tt in the following form:

$$D_\mathrm{y} = K_\mathrm{p} \cdot \sqrt{Tt} \tag{5.54}$$

K_p is a polymer-specific constant. The yarn diameter D_y will be reached in the unit of m, if Tt is set in tex and for K_p the following values are set at:

$K_\mathrm{p} = 33.3 \cdot 10^{-6}$ for the fibre material PA (density = 1.12 g/cm^3)
$K_\mathrm{p} = 30 \cdot 10^{-6}$ for the fibre material PET (density = 1.38 g/cm^3)

The final mathematic-dynamic model equation of the twist density T_D can be calculated now on the basis of DEq. 5.44 and under the consideration of the Eqs. 5.53 and 5.54 as follows:

$$\Phi = n_\mathrm{s} - T_\mathrm{D} \cdot \sqrt{[(v_\mathrm{o} - v_\mathrm{z}) \cdot \exp(-\mu\alpha_\mathrm{m}) + v_\mathrm{z}]^2 - Tt(\pi K_\mathrm{p} \cdot n_\mathrm{s})^2} - p \cdot T_\mathrm{D} \cdot l_\mathrm{m} = 0 \tag{5.55}$$

Differential equation 5.55 can be partially derived (for the purpose of its linearisation) from the potentially changeable variables T_D, n_s, v_z, v_o, Tt and μ according to the already often demonstrated manner:

$$\frac{\partial\Phi}{\partial T_\mathrm{D}} \cdot \Delta T_\mathrm{D} + \frac{\partial\Phi}{\partial n_\mathrm{s}} \cdot \Delta n_\mathrm{s} + \frac{\partial\Phi}{\partial v_\mathrm{z}} \cdot \Delta v_\mathrm{z} + \frac{\partial\Phi}{\partial v_\mathrm{o}} \cdot \Delta v_\mathrm{o} + \frac{\partial\Phi}{\partial Tt} \cdot \Delta Tt + \frac{\partial\Phi}{\partial \mu} \cdot \Delta\mu = 0$$

If the partial differentiations are carried out then one gets the linearised DEq. of the twist density T_D as follows. It should be considered through this that $T_\mathrm{Dm} = n_\mathrm{Dm}/W_\mathrm{a}$

$$\begin{aligned}
&\left[\frac{W_\mathrm{a}^2}{n_\mathrm{sm}} + Tt_\mathrm{m} \cdot n_\mathrm{sm}(\pi K_\mathrm{p})^2\right] \cdot \Delta n_\mathrm{s} - \langle N_\mathrm{a}[1 - \exp(-\mu_\mathrm{m}\alpha_\mathrm{m})]\rangle \cdot \Delta v_\mathrm{z} \\
&- N_\mathrm{a} \cdot \exp(-\mu_\mathrm{m}\alpha_\mathrm{m}) \cdot \Delta v_\mathrm{o} + 0.5 \cdot (\pi K_\mathrm{p} \cdot n_\mathrm{sm})^2 \cdot \Delta Tt \\
&+ [\alpha_\mathrm{m} \cdot N_\mathrm{a}(v_\mathrm{om} - v_\mathrm{zm}) \cdot \exp(-\mu_\mathrm{m}\alpha_\mathrm{m})] \cdot \Delta\mu - \frac{W_\mathrm{a}^2}{n_\mathrm{sm}}[W_\mathrm{a} + p \cdot l_\mathrm{m}] \cdot \Delta T_\mathrm{D} = 0
\end{aligned} \tag{5.56}$$

The abbreviations W_a and N_a mean:

$$W_\mathrm{a} = \sqrt{[(v_\mathrm{om} - v_\mathrm{zm}) \cdot \exp(-\mu_\mathrm{m}\alpha_\mathrm{m}) + v_\mathrm{zm}]^2 - Tt_\mathrm{m}(\pi K_\mathrm{p} \cdot n_\mathrm{sm})^2} \tag{5.57}$$

$$N_\mathrm{a} = (v_\mathrm{om} - v_\mathrm{zm}) \cdot \exp(-\mu_\mathrm{m}\alpha_\mathrm{m}) + v_\mathrm{zm} \tag{5.58}$$

Equation 5.56 can be used now to calculate the *dynamic transfer functions*, which inform about the influence of Δn_s-, Δv_z-, Δv_o-, ΔTt-, or $\Delta\mu$- changes to changes of the twist density ΔT_D:

$$G_1(p) = \frac{\Delta T_\mathrm{D}}{\Delta n_\mathrm{s}} = \frac{\dfrac{W_\mathrm{a}^2}{n_\mathrm{sm}} + Tt_\mathrm{m} \cdot n_\mathrm{sm}(\pi K_\mathrm{p})^2}{\dfrac{W_\mathrm{a}^2}{n_\mathrm{sm}}(W_\mathrm{a} + p \cdot l_\mathrm{m})} \tag{5.59}$$

$$G_2(p) = \frac{\Delta T_\mathrm{D}}{\Delta v_\mathrm{z}} = -\frac{N_\mathrm{a}[1 - \exp(-\mu_\mathrm{m}\alpha_\mathrm{m})]}{\dfrac{W_\mathrm{a}^2}{n_\mathrm{sm}}(W_\mathrm{a} + p \cdot l_\mathrm{m})} \tag{5.60}$$

$$G_3(p) = \frac{\Delta T_\mathrm{D}}{\Delta v_\mathrm{o}} = -\frac{N_\mathrm{a} \cdot \exp(-\mu_\mathrm{m}\alpha_\mathrm{m})}{\dfrac{W_\mathrm{a}^2}{n_\mathrm{sm}}(W_\mathrm{a} + p \cdot l_\mathrm{m})} \tag{5.61}$$

$$G_4(p) = \frac{\Delta T_\mathrm{D}}{\Delta Tt} = \frac{0.5(\pi K_\mathrm{p} \cdot n_\mathrm{sm})^2}{\dfrac{W_\mathrm{a}^2}{n_\mathrm{sm}}(W_\mathrm{a} + p \cdot l_\mathrm{m})} \tag{5.62}$$

$$G_5(p) = \frac{\Delta T_\mathrm{D}}{\Delta \mu} = \frac{\alpha_\mathrm{m} \cdot N_\mathrm{a}(v_\mathrm{om} - v_\mathrm{zm}) \cdot \exp(-\mu_\mathrm{m}\alpha_\mathrm{m})}{\dfrac{W_\mathrm{a}^2}{n_\mathrm{sm}}(W_\mathrm{a} + p \cdot l_\mathrm{m})} \tag{5.63}$$

The corresponding normalised *amplitude frequency responses* of these transfer functions (all of them show proportional action with delay of first order) are the following:

$$|G_1(\mathrm{j}f)| = \left| \frac{\widetilde{\Delta T_\mathrm{D}}/T_\mathrm{Dm}}{\widetilde{\Delta n_\mathrm{s}}/n_\mathrm{sm}} \right| = \frac{W_\mathrm{a}^2 + Tt_\mathrm{m}(\pi K_\mathrm{p} \cdot n_\mathrm{sm})^2}{W_\mathrm{a}\sqrt{W_\mathrm{a}^2 + (2\pi f \cdot l_\mathrm{m})^2}} \tag{5.64}$$

$$|G_2(\mathrm{j}f)| = \left| \frac{\widetilde{\Delta T_\mathrm{D}}/T_\mathrm{Dm}}{\widetilde{\Delta v_\mathrm{z}}/v_\mathrm{zm}} \right| = (-)\frac{v_\mathrm{zm} \cdot N_\mathrm{a}[1 - \exp(-\mu_\mathrm{m}\alpha_\mathrm{m})]}{W_\mathrm{a}\sqrt{W_\mathrm{a}^2 + (2\pi f \cdot l_\mathrm{m})^2}} \tag{5.65}$$

$$|G_3(\mathrm{j}f)| = \left| \frac{\widetilde{\Delta T_\mathrm{D}}/T_\mathrm{Dm}}{\widetilde{\Delta v_\mathrm{o}}/v_\mathrm{om}} \right| = (-)\frac{v_\mathrm{om} \cdot N_\mathrm{a} \cdot \exp(-\mu_\mathrm{m}\alpha_\mathrm{m})}{W_\mathrm{a}\sqrt{W_\mathrm{a}^2 + (2\pi f \cdot l_\mathrm{m})^2}} \tag{5.66}$$

$$|G_4(\mathrm{j}f)| = \left| \frac{\widetilde{\Delta T_\mathrm{D}}/T_\mathrm{Dm}}{\widetilde{\Delta Tt}/Tt_\mathrm{m}} \right| = \frac{0.5 \cdot Tt_\mathrm{m}(\pi K_\mathrm{p} \cdot n_\mathrm{sm})^2}{W_\mathrm{a}\sqrt{W_\mathrm{a}^2 + (2\pi f \cdot l_\mathrm{m})^2}} \tag{5.67}$$

$$|G_5(\mathrm{j}f)| = \left| \frac{\widetilde{\Delta T_\mathrm{D}}/T_\mathrm{Dm}}{\widetilde{\Delta \mu}/\mu_\mathrm{m}} \right| = \frac{\mu_\mathrm{m} \cdot \alpha_\mathrm{m} \cdot N_\mathrm{a}(v_\mathrm{om} - v_\mathrm{zm}) \cdot \exp(-\mu_\mathrm{m}\alpha_\mathrm{m})}{W_\mathrm{a}\sqrt{W_\mathrm{a}^2 + (2\pi f \cdot l_\mathrm{m})^2}} \tag{5.68}$$

The corresponding *phase frequency response* of the *complex frequency responses* $G_1(\mathrm{j}f)$, $G_4(\mathrm{j}f)$ and $G_5(\mathrm{j}f)$ are uniformly:

$$\varphi(f) = \operatorname{arc\,tan}\left[-\frac{2\pi f \cdot l_\mathrm{m}}{W_\mathrm{a}}\right] \tag{5.69}$$

The corresponding *phase frequency response* of the *complex frequency responses* $G_2(\mathrm{j}f)$ and $G_3(\mathrm{j}f)$ are:

$$\varphi(f) = \text{arc tan}\left[-\frac{2\pi f \cdot l_\mathrm{m}}{W_\mathrm{a}}\right] - \pi \tag{5.70}$$

An incidental evaluation of the achieved equations should be undertaken at this point before we can discuss a quantitative result presentation of a technological process example:

a) In each case, the amplitude transmission factors of Eqs. 5.64 to 5.68 do not only depend on the disturbance frequency f but also, strongly, on the mean values of the independent process and product variables which define the viewed technological operation point. This is an expression for the declared complexity of the investigated general problem in spite of the simplifications and neglects made in the statements.

b) The time constant T_c and the critical frequency f_c of the process line are qualitatively the same for all kinds of viewed disturbances and depend likewise on the mean values of all independent process and product variables. They can be best written from the phase frequency response Eq. 5.70 (see to this Sect. 4.2.1):

$$\frac{1}{2\pi f_\mathrm{c}} = T_\mathrm{c} = \frac{l_\mathrm{m}}{W_\mathrm{a}} \tag{5.71}$$

The abbreviation W_a (see Eq. 5.57) is identical with the yarn velocity in the texturing and setting zone.

c) The parameter W_a allows the data of a limit condition. This is not allowed to be exceeded if a proper thread line (that really means the carrying out of the process) should be reached. This deals with the yarn tensile stress, yarn velocity and yarn twist density relations. This limited condition can be defined as maximum eligible speed of the false twist spindle n_sm dependent upon the other free eligible process and product variables. They can be derived from the trivial condition that the radicand of the root (Eq. 5.57) is not allowed to be negative. It must always be fulfilled as:

$$n_\mathrm{sm} \leq \frac{(v_\mathrm{om} - v_\mathrm{zm}) \cdot \exp(-\mu_\mathrm{m}\alpha_\mathrm{m}) + v_\mathrm{zm}}{\pi \cdot K_\mathrm{p} \cdot \sqrt{T t_\mathrm{m}}} \tag{5.72}$$

The following dimensions are to be inserted in Eqs. 5.53 to 5.72 for quantitative calculations:

$v_{\mathrm{om}}, v_{\mathrm{zm}}$	numerical values to put in m/min
n_{sm}	numerical values to put in min^{-1}
l_{m}	numerical values to put in m
Tt_{m}	numerical values to put in tex
f	numerical values to put in min^{-1} or 60Hz
K_{p}	numerical values to put in as described in Eq. 5.54
α_{m}	numerical values to put in the radian measure (dimensionless)
μ_{m}	coefficient of friction (dimensionless)

Technological Application and Analysis

At first Fig. 5.23 shows the limit curves of the eligible revolutions per minute of the false twist spindle n_{sm} for the fine yarn range (2 until 20 tex) and dependent upon different velocity and angle of wrap levels for the fibre materials PA and PET. These correspond to the further investigated technological variants which are collected in Table 5.1.

The curves confirm the practical experiences that the eligible (and also necessary to reach an appointed twist density T_{Dm}) speed of the false twist spindle n_{sm} increases if the fineness Tt_{m} decreases and the yarn take-up velocity v_{om} increases. It is to be remarked that the results have the correct size. The latter is moreover an indirect proof for the exactness for the principle of the selected model idea.

Relating to practice, variants of the process realisation have been selected for detailed analysis by means of the developed model equations. They have been collected in Table 5.1 considering the preliminary investigations. The last two columns contain the time constants T_{c} and the critical frequencies f_{c} of the texturing and setting zone which roughly characterise the dynamic transmission behaviour.

The time constants T_{c} amount to about 2.50 s for the velocity level 100 m/min and about 1.65 s for the velocity level 200 m/min (indeed with an assumed increased length of $l_{\mathrm{m}} = 4$ m). It can be concluded from this that aperiodic disturbances of the viewed process and product variables will effect undefined bulkiness properties along a thread length of about 12 m in the first case ($v_{\mathrm{om}} = 100$ m/min) and of about 17 m in the second case ($v_{\mathrm{om}} = 200$ m/min).

The small critical frequencies f_{c} of about 0.065 Hz at $v_{\mathrm{om}} = 100$ m/min and of about 0.1 Hz at $v_{\mathrm{om}} = 200$ m/min mean that periodic disturbances of only relatively small frequency will have a considerable influence on the twist density $\widetilde{\Delta T_{\mathrm{D}}}$. Frequencies > 0.5 Hz will already have a sufficient dampening in each case. The following figures also show this.

The normalised amplitude frequency responses $|G_1(\mathrm{j}f)|$ to $|G_5(\mathrm{j}f)|$ are presented in Figs. 5.24 to 5.28 for all technological variants according to Table 5.1.

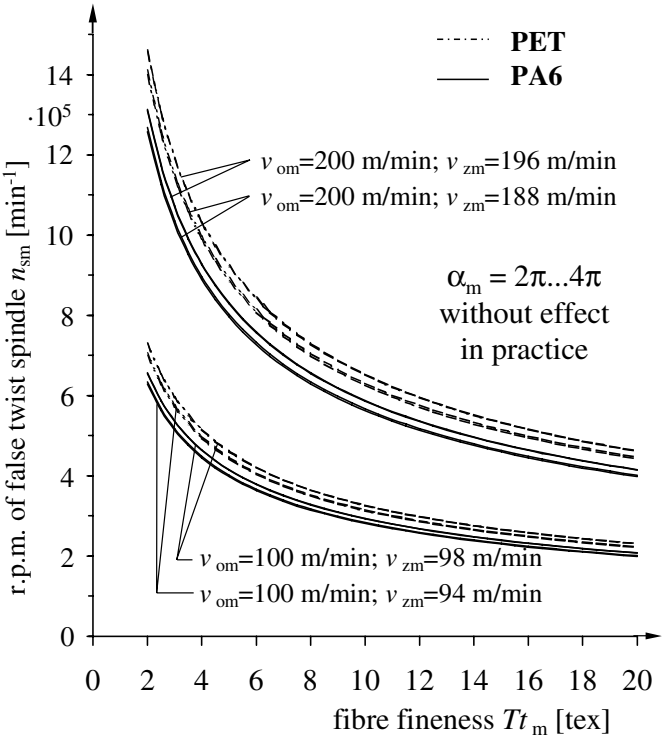

Fig. 5.23. Limit curves of eligible revolutions per minute of the false twist spindle n_{sm} dependent upon different technological conditions according to Eq. 5.72. Further data see Table 5.1

Comparing the study of the figures leads to the following general conclusions for the disturbance estimation:

a) Speed changes of the twisting element $\widetilde{\Delta n_s}$ have the greatest effect on the twist density T_D ($|G_1(jf)|$, Fig. 5.24). Relative amplification factors of 1.0 to 2.0 will be reached in the disturbance frequency range $f < f_c$. This means that $\widetilde{\Delta n_s}$-changes of 1% can effect $\widetilde{\Delta T_D}$-changes from 1 to 2%. The finenesses of the texturised thread Tt_m are of only small influence, in which the coarser thread will be influenced more (specifically at the quasi steady state disturbances – f nearly 0 Hz) than the finer. The usual variations of the thread input velocity v_z relative to the thread output velocity v_o (present lags are assumed from –2% to –6%) and number of wraps around the pin of the twisting element (assumed 1 or 2 wraps) practically have no influence on the start height of the curves and their further courses. On the other hand, a PA-thread will be influenced more strongly than a PET-thread of the same fineness.

Table 5.1. Technological variants of the investigated FT-texturing process

Process variant	v_{om} in m/min	v_{zm} in m/min	T_{Dm} in m^{-1}	n_{sm} in m^{-1}	α_m	μ_m	K_p	Tt_m in tex	l_m in m	T_c in s	f_c in Hz
							PA-fibres				
1	100	98	4300	325348	2π	0.3	$33.3 \cdot 10^{-6}$	3.4	3.0	2.38	0.067
2	100	94	4300	314120	2π	0.3	$33.3 \cdot 10^{-6}$	3.4	3.0	2.46	0.065
3	100	98	4300	324496	4π	0.3	$33.3 \cdot 10^{-6}$	3.4	3.0	2.39	0.067
4	100	94	4300	311562	4π	0.3	$33.3 \cdot 10^{-6}$	3.4	3.0	2.48	0.064
							PA-fibres				
5	100	98	3000	221776	2π	0.3	$33.3 \cdot 10^{-6}$	7.8	3.0	2.43	0.065
6	100	94	3000	214122	2π	0.3	$33.3 \cdot 10^{-6}$	7.8	3.0	2.52	0.063
7	100	98	3000	221195	4π	0.3	$33.3 \cdot 10^{-6}$	7.8	3.0	2.44	0.065
8	100	94	3000	212379	4π	0.3	$33.3 \cdot 10^{-6}$	7.8	3.0	2.54	0.063
							PET-fibres				
9	100	98	3000	232598	2π	0.3	$30.0 \cdot 10^{-6}$	7.6	3.0	2.32	0.069
10	100	94	3000	224570	2π	0.3	$30.0 \cdot 10^{-6}$	7.6	3.0	2.40	0.066
11	100	98	3000	231988	4π	0.3	$30.0 \cdot 10^{-6}$	7.6	3.0	2.33	0.068
12	100	94	3000	222742	4π	0.3	$30.0 \cdot 10^{-6}$	7.6	3.0	2.42	0.066
							PET-fibres				
13	100	98	2300	169244	2π	0.3	$30.0 \cdot 10^{-6}$	16.7	3.0	2.45	0.065
14	100	94	2300	163403	2π	0.3	$30.0 \cdot 10^{-6}$	16.7	3.0	2.53	0.063
15	100	98	2300	168800	4π	0.3	$30.0 \cdot 10^{-6}$	16.7	3.0	2.45	0.065
16	100	94	2300	162072	4π	0.3	$30.0 \cdot 10^{-6}$	16.7	3.0	2.55	0.062
							PA-fibres				
17	200	196	4300	650696	2π	0.3	$33.3 \cdot 10^{-6}$	3.4	4.0	1.59	0.100
18	200	188	4300	628240	2π	0.3	$33.3 \cdot 10^{-6}$	3.4	4.0	1.64	0.097
19	200	196	4300	648992	4π	0.3	$33.3 \cdot 10^{-6}$	3.4	4.0	1.59	0.100
20	200	188	4300	623125	4π	0.3	$33.3 \cdot 10^{-6}$	3.4	4.0	1.66	0.096
							PA-fibres				
21	200	196	3000	443552	2π	0.3	$33.3 \cdot 10^{-6}$	7.8	4.0	1.62	0.098
22	200	188	3000	428244	2π	0.3	$33.3 \cdot 10^{-6}$	7.8	4.0	1.68	0.095
23	200	196	3000	442390	4π	0.3	$33.3 \cdot 10^{-6}$	7.8	4.0	1.63	0.098
24	200	188	3000	424757	4π	0.3	$33.3 \cdot 10^{-6}$	7.8	4.0	1.70	0.094
							PET-fibres				
25	200	196	3000	465196	2π	0.3	$30.0 \cdot 10^{-6}$	7.6	4.0	1.55	0.103
26	200	188	3000	449141	2π	0.3	$30.0 \cdot 10^{-6}$	7.6	4.0	1.60	0.099
27	200	196	3000	463977	4π	0.3	$30.0 \cdot 10^{-6}$	7.6	4.0	1.55	0.103
28	200	188	3000	445484	4π	0.3	$30.0 \cdot 10^{-6}$	7.6	4.0	1.62	0.098
							PET-fibres				
29	200	196	2300	338487	2π	0.3	$30.0 \cdot 10^{-6}$	16.7	4.0	1.63	0.098
30	200	188	2300	326806	2π	0.3	$30.0 \cdot 10^{-6}$	16.7	4.0	1.69	0.094
31	200	196	2300	337600	4π	0.3	$30.0 \cdot 10^{-6}$	16.7	4.0	1.64	0.097
32	200	188	2300	324145	4π	0.3	$30.0 \cdot 10^{-6}$	16.7	4.0	1.70	0.093

b) Changes $\widetilde{\Delta v_z}$ effect changes $\widetilde{\Delta T_D}$ quantitatively in the same manner ($|G_2(\mathrm{j}f)|$, Fig. 5.25). Amplification factors of 1.0 to 1.9 are also to be observed in the frequency range $f < f_c$ for such disturbances.
Smaller differences are given as follows: The coarser thread and the thread with the greater number of wraps around the pin of the twisting element will be disturbed relatively stronger than the finer thread and the thread with only one wrap around the pin ($\alpha_m = 2\pi$). PA-threads are more disturbance endangered than PET-threads. The influence of the lag of v_{zm} is relatively

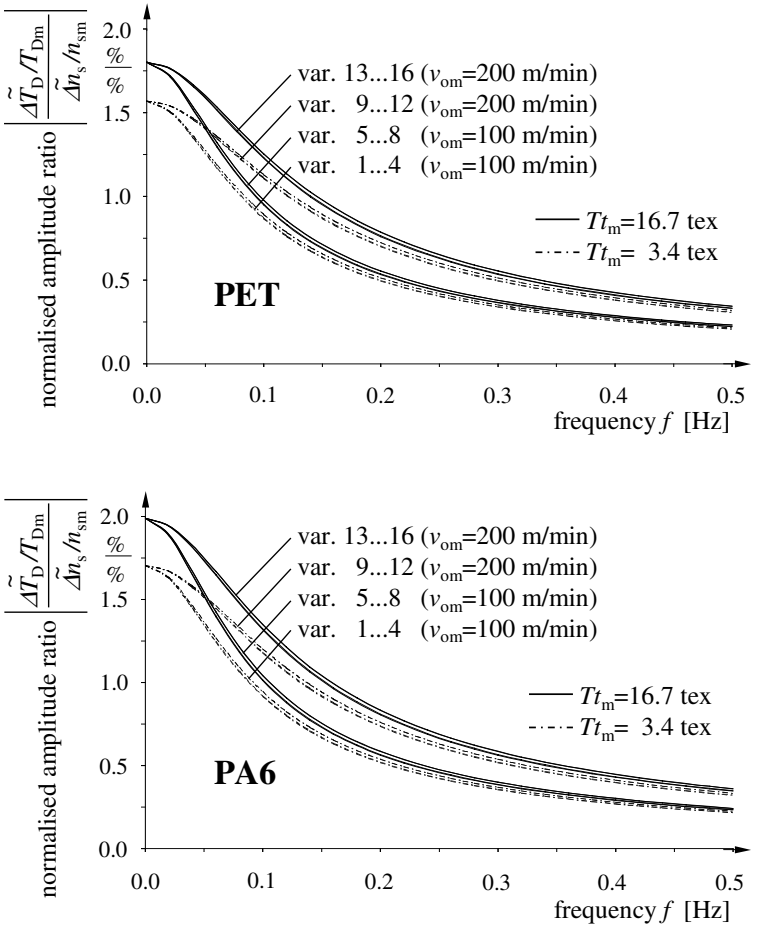

Fig. 5.24. Normalised amplitude frequency responses of twist density changes $\widetilde{\Delta T_D}$ caused by changes of the false twist spindle speed $\widetilde{\Delta n_s}$ at the FT-texturing process. Further data see Table 5.1

insignificant; the variants with –6% lag have only somewhat lower amplitude frequency response curves than those with –2% lag.

c) The output velocity v_o clearly influences the goal variable $\widetilde{\Delta T_D}$ less than the process variables n_s and v_z, named under a) and b) ($|G_3(jf)|$, Fig. 5.26). Changes $\widetilde{\Delta v_o}$ reach relative amplitude amplification factors of < 0.32, that means a more than 3% periodic change of $\widetilde{\Delta v_o}$ around its mean value v_{om} will effect a 1% periodic change of the twist density $\widetilde{\Delta T_D}$ in an appropriately small frequency range. A clear separation of the curves dependent on the angle of wrap α_m appears as well. The amplification factors nearly reach 0.32 (PA 6)

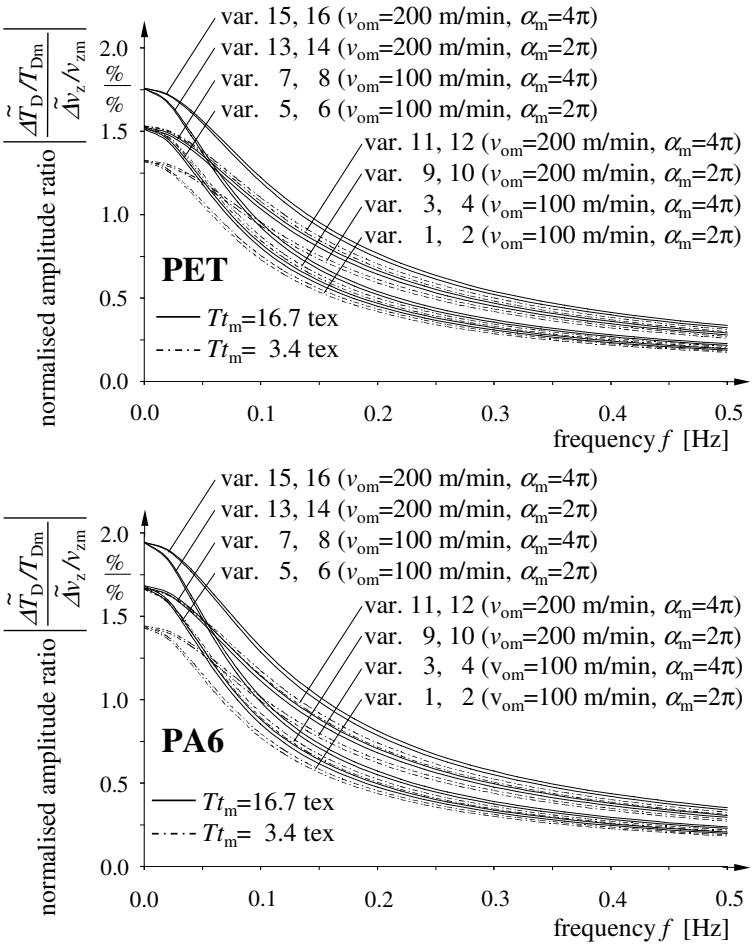

Fig. 5.25. Normalised amplitude frequency responses of twist density changes $\widetilde{\Delta T_D}$ caused by changes of the input velocity $\widetilde{\Delta v_z}$ at the FT-texturing process. Further data see Table 5.1

for 1 wrap around the pin of the twisting element and they only reach insignificant values of 0.05 for 2 wraps. Smaller insignificant differences can be observed as follows: The process with the greater lag of v_{zm} opposite v_{om} and the coarser threads show somewhat greater disturbance transmission factors. PA is to be assessed again more unfavourably than PET.

This total result is also physical-obviously plausible so far, as output velocity changes must be transmitted into the texturing and setting zone of the friction wrap line at first which effects dampening in this case. The output velocity changes are effective only indirectly to the change $\widetilde{\Delta T_D}$ of the influence of the real velocity pertaining to the twisted thread v_i (see Eq. 5.57,

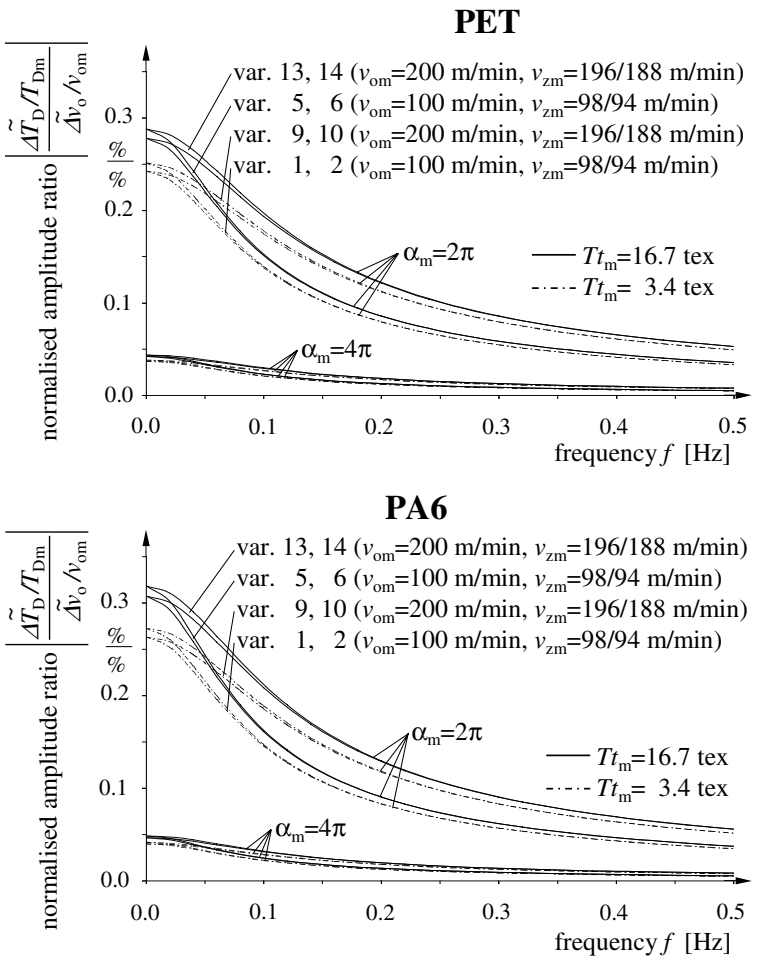

Fig. 5.26. Normalised amplitude frequency responses of twist density changes $\widetilde{\Delta T_D}$ caused by changes of the output velocity $\widetilde{\Delta v_o}$ at the FT-texturing process. Further data see Table 5.1

abbreviation W_a is identical with v_{im}). It is intelligible that a lengthening of this dampening friction thread line additionally degrades the influence of $\widetilde{\Delta v_o}$ to $\widetilde{\Delta T_D}$ drastically.

d) Also the fineness of the texturising thread Tt and its changes $\widetilde{\Delta Tt}$ effect changes of the twist density $\widetilde{\Delta T_D}$ only with a maximum amplitude transmission factor of 0.3 to 0.5 ($|G_4(jf)|$, Fig. 5.27). The curves obviously show the larger, more unfavourable, values for coarser threads and (frequently pointed out previously) for PA compared to PET.

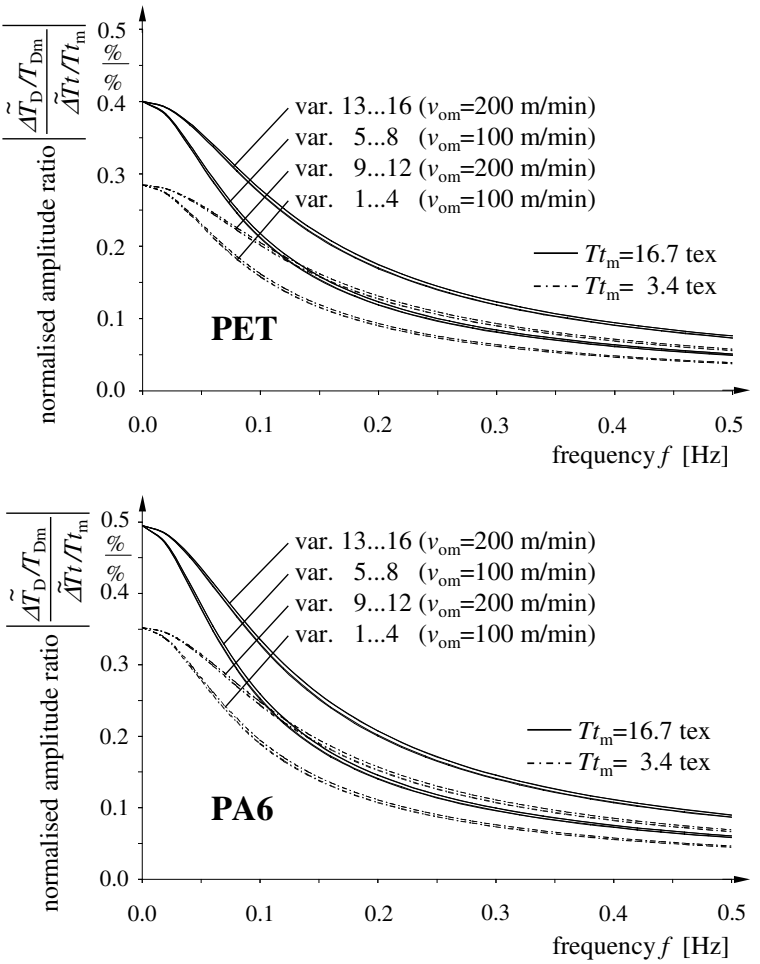

Fig. 5.27. Normalised amplitude frequency responses of twist density changes $\widetilde{\Delta T_D}$ caused by changes of the thread fineness $\widetilde{\Delta Tt}$ at the FT-texturing process. Further data see Table 5.1

e) The system behaviour regarding to changes $\widetilde{\Delta\mu}$ and their effect on changes $\widetilde{\Delta T_D}$ ($|G_5(jf)|$) is demonstrated in Fig. 5.28. The amplitude transmission factors are extremely small with ≤ 0.04 for which a great angle of wrap and/or a small v_z-lag causes a further drastic decrease. Changes $\widetilde{\Delta\mu}$ of about 30 to 40% would be necessary to effect a 1% change $\widetilde{\Delta T_D}$. This is to be practically excluded. But, it is to be remarked additionelly, that the present model comprises changes $\widetilde{\Delta\mu}$ which only effect twist density changes by means of velocity changes $\widetilde{\Delta v_i}$ of the texturised thread. Effects are not included, on the other hand, which twist slip appearences at the pin of the twisting ele-

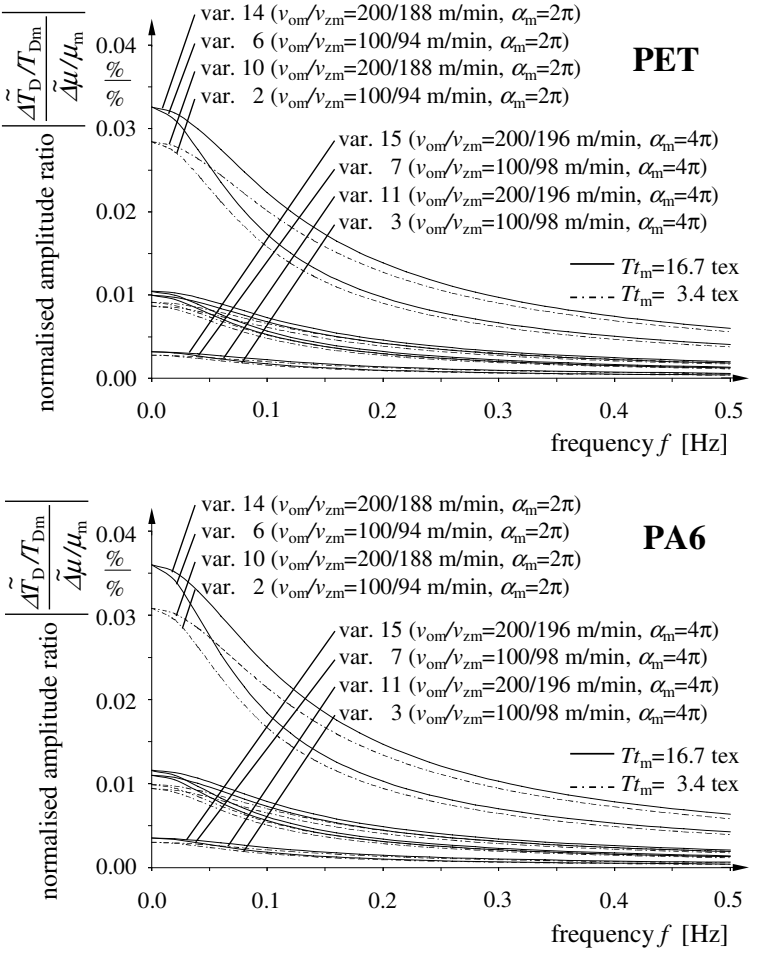

Fig. 5.28. Normalised amplitude frequency responses of twist density changes $\widetilde{\Delta T_\mathrm{D}}$ caused by changes of the friction coefficient $\widetilde{\Delta\mu}$ at the FT-texturing process. Further data see Table 5.1

ment (missing friction adhesion) evoked by means of great changes to $\widetilde{\Delta\mu}$. Of course, these twist slip appearences possibly effect much greater twist density changes but they are not covered by the chosen model.

The common valid phase frequency response curves for the dynamic transmission functions $G_1(p)$ to $G_5(p)$ (Eqs. 5.69 and 5.69) are shown in Fig. 5.29 for all technological variants according to Table 5.1. The delay thread length L_d can be calculated by means of these because this has been demonstrated in Sect. 5.1.5 (see also Eq. 2.50). The length L_d represented in the present example which thread length leaves the texturing and setting zone before a

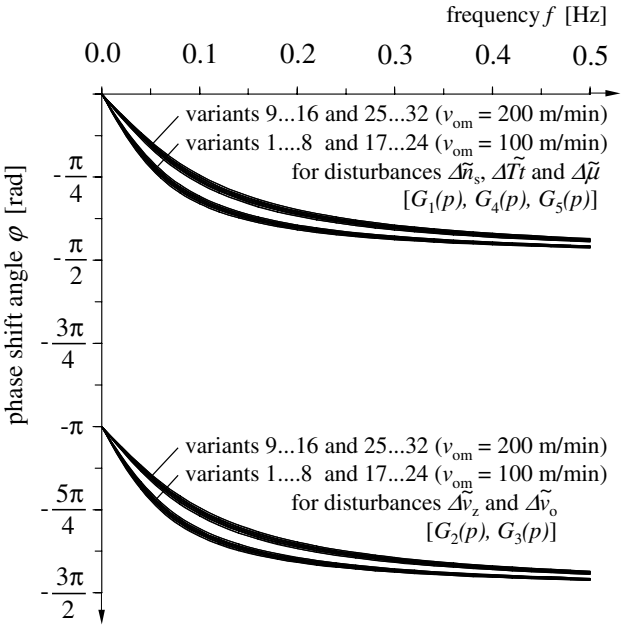

Fig. 5.29. Phase frequency responses of twist density changes $\widetilde{\Delta T_\mathrm{D}}$ caused by changes of all regarded disturbance quantities at the FT-texturing process. Further data see Table 5.1

change $\widetilde{\Delta n_\mathrm{s}}$, $\widetilde{\Delta v_\mathrm{o}}$, $\widetilde{\Delta v_\mathrm{z}}$, $\widetilde{\Delta T t}$ or $\widetilde{\Delta \mu}$ will or can be visible in the output thread as changes $\widetilde{\Delta T_\mathrm{D}}$. It has already been mentioned before that certain correlations exist here with the time constant T_c or the critical frequency f_c.

Two remarks should be given at the end of this subsection to the transmission of the presented model to other process realisations of the FT-texturing:

1. All model equations should also be transmittable to the friction texturing process considering the developed imaginations and derivations in Sects. 5.1.4 and 5.1.5, if

a) the angle of wrap α_m is interpreted as the sum of single angles which are imprinted repeatedly to the thread by means of the friction disk. The friction unit is assumed to be a collected effect at this point.

b) the efficiency of the twist transmission from the twisting element to the thread[1] is considered in the DEqs. 5.44 or 5.56 to be in the form of $0.7 \cdot T_\mathrm{D}$, $0.7 \cdot T_\mathrm{Dm}$ or $0.7 \cdot \Delta T_\mathrm{D}$. The normalised results of Eqs. 5.64 to 5.68 are then applicable in the same manner.

[1] It is usually realised for the magnetic spindle principle with 100%; the efficiency is only $\leq 70\%$ for the friction principle

2. The model seems to be more problematic to transmit to a simultaneous draw-texturing process because twist generation and drawing are superimposed here. It should additionally be considered that the heating of the thread (not considered until here) well-known decreases the mechanical draw energy in the thread. Much harder conceivable relations are already given under pure steady state view.
A coarse approximation of the real situation for the dynamic model could be that one modifies Eqs. 5.53 and 5.57 as follows:

a) The input velocity of the partial else to drawing thread v_z is to be corrected by multiplying it with the draw ratio which is realised in the texturing and setting zone. This product, named v_{zc}, is then (instead of v_z) the basis for the calculation of the velocity v_i which appoints the twist density.

b) It is generally to be inserted in the fineness and the diameter of the drawn thread only.

5.3 Dynamics of Fibre Heating and Cooling

5.3.1 Task

The mathematical description of lapses of thermic proceedings is of importance in the modelling of appointed fibre formation and processing processes. This becomes true specifically for process stages of manufacturing and processing processes of polymer threads. The fibre formation of melts, the draw process (if thermic energy is induced), and the texturing are examples of this. Heating as well as cooling processes are to be described for the modelling of the temperature-time-courses in the thread.

Thread heating and cooling processes are effected by means of *heat spreading processes* which are due to three different basic principles:

a) *Heat conduction* which is to be described as heat spreading in solid, resting fluid and resting gaseous bodies from points of higher temperature to points of lower temperature.

b) *Heat convection* or *heat transfer* which is to be described as heat transport by means of flowing fluids or flowing gases which is to be distinguished between the *enforced* convection (flow separately generated) and the *free* convection (flow arises from itself by means of density or pressure differences).

c) *Heat radiation* which is to be described as heat transfer between bodies by means of electro-magnetic waves of the infrared spectral range without the co-operation of a transmission medium.

All three principles are effective for the thread heating depending on the process stage, for the thread cooling essentially only the principles a) and b).

The *convection* or the *heat transfer* is of *essential importance* to the calculation – and with this the modelling – of heating and cooling processes of running threads in fibre formation lines of melt spinning processes, around the heated or unheated godet systems and in texturing heaters.

Questions relating to such dynamic models can be for instance:

a) At which distance from the spinneret and under which conditions a melt spun thread will be solidified?
b) How many thread wraps around a heated godet or a system of such godets are necessary (for appointed boundary conditions, for instance thread fineness, thread velocity, godet geometry), that a maximum possible thread temperature can be reached?
c) How high is the reached mean thread temperature (under given boundary conditions) in relation to the godet temperature?
d) How large are the fluctuations of the thread temperature of the mean value which the thread suffers at one wrap around the godet system.

The answer to those questions is necessary for an optimal process operation as well as to the design of machine elements. In the following a simplified description of the heat transfer between a thread and its surrounding which enables process applied calculations with sufficient exactness as a rule will be given. The heat transfer between threads and metallic surfaces and between threads and air is theoretically explained in more detail in the additional literature [311] to [313] considering heat transfer and heat equalise proceedings in a monofilament thread on the one hand and multifilament threads on the other. However, the study shows that appropriate results and methods are not applicable enough for engineers in practice and are also difficult to handle.

5.3.2 Differential Equation for the Description of Heat Transfer at Fibres

Starting point of the view is the common DEq. of the heat exchange processes on the surface of a cylindrical body, and without consideration of the heat conduction inside the body. The last assumption means an equal temperature across the whole thread cross section[2]. In other words, there is no temperature

[2] This assumption is fulfilled not in any practical case because an utter heating or cooling of the thread (general body) assumes a heat flow (being due to the heat conduction principle) from the surface to the core or vice versa. Nevertheless, temperature differences are just the impulse for this. But, these differences amount only to a few *Kelvin* for threads with their big surface-volume-ratios (for coarse threads more unfavourable than for fine) and they are very small compared to the normally imprinted mean temperature changes. Therefore this assumption does not involve aggravating mistakes.

difference between core and surface of the radial symmetric thread cross section. If the heat balance is viewed on a small disk of a cylindrical thread piece according to Fig. 5.30 then for heating [314] is valid

$$c \cdot \mathrm{d}m \cdot \mathrm{d}T_\mathrm{y} = \alpha \cdot \mathrm{d}S_\mathrm{y} \cdot (T_\mathrm{h} - T_\mathrm{y}) \cdot \mathrm{d}t \tag{5.73}$$

the left side of Eq. 5.73: absorbed heat quantity
the right side of Eq. 5.73: about the surface transmitted heat quantity

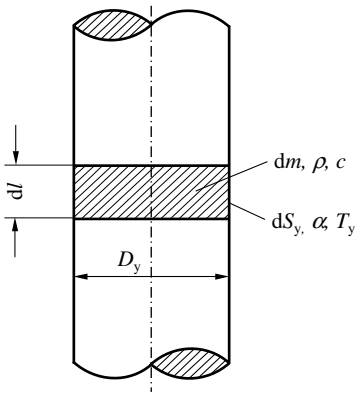

Fig. 5.30. Cylindrical thread piece

In Fig. 5.30 and Eq. 5.73 the symbols mean:

$\mathrm{d}S_\mathrm{y}$	surface of the disk-shaped thread piece which takes part in the heat exchange
D_y	diameter of the thread piece
$\mathrm{d}l$	length of the thread piece
$\mathrm{d}m$	mass of the thread piece
ϱ	density of the thread material
c	specific heat capacity of the thread material
α	coefficient of the heat transfer
T_y	temperature of the thread piece
T_h	temperature of the heat medium
$\mathrm{d}t$	time interval for the heat exchange
$\mathrm{d}T_\mathrm{y}$	temperature change of the thread piece

The following mass-surface-ratio is valid for the cylindrical- or disk-shaped thread piece

$$\frac{\mathrm{d}m}{\mathrm{d}S_\mathrm{y}} = \frac{\pi \cdot D_\mathrm{y}^2 \cdot \varrho \cdot \mathrm{d}l}{4 \cdot \pi \cdot D_\mathrm{y} \cdot \mathrm{d}l} = \frac{D_\mathrm{y} \cdot \varrho}{4} \tag{5.74}$$

The DEq. 5.73 can be simply integrated considering Eq. 5.74

$$\int_{T_b}^{T_y} \frac{dT_y}{T_h - T_y} = \int_0^t \frac{4 \cdot \alpha}{c \cdot \varrho \cdot D_y} \cdot dt \tag{5.75}$$

The equation for the *fibre heating* results from Eq. 5.75 to

$$T_y = T_h - (T_h - T_b) \cdot \exp\left(-\frac{4 \cdot \alpha}{c \cdot \varrho \cdot D_y} \cdot t\right) \tag{5.76}$$

T_b is the thread temperature at the beginning of the heat exchange, that means to the time $t = 0$.

The DEq. 5.73 can be similarly solved for the thread cooling from the temperature at the beginning of the heat exchange T_b in a surrounding cool medium with the temperature T_r.

The equation for the *fibre cooling* can be read as:

$$T_y = T_r + (T_b - T_r) \cdot \exp\left(-\frac{4 \cdot \alpha}{c \cdot \varrho \cdot D_y} \cdot t\right) \tag{5.77}$$

Eqations 5.76 and 5.77 describe the thread heating and cooling as a dynamic transfer process (in the form of the step response function) in a approximated, but simplified manner. The practical use and the application of these equations to monofilament as well as multifilament man-made yarns are shown in the following: The thread diameter D_y of a multifilament yarn is to be calculated from its fineness (not from the fineness of the single filament!) as the equivalent diameter which would have a monofilament yarn of the same fineness [315]. This equivalent diameter (which has been proven correct for the heat transfer) is:

$$D_y = \sqrt{\frac{4 \cdot Tt}{\varrho \cdot \pi \cdot 10^9}} \tag{5.78}$$

The following dimensions are to be inputted:

fineness of the whole thread Tt in tex
density of the fibre material ϱ in g/cm^3

The equivalent diameter of the whole thread D_y will be obtained in m.

Equation 5.78 has already been used in Sect. 5.2.2 as a numerical value equation. All numerical constants for the fibre materials PA and PET (including the densities ϱ) have been collected to the numerical constants K_p (see Eq. 5.54).

For user friendly style of writing of the Eqs. 5.76 and 5.77 it is recommended here that the material specific constants c and ϱ, as well as all numerical constants in the exponent of the e-functions (which remain after the substitution of the diameter D_y by the fineness Tt according to Eq. 5.78), are collected to a material specific constant for the heat transfer K_h.

The equations can now be read as follows:

For the *fibre heating*:

$$T_\mathrm{y} = T_\mathrm{h} - (T_\mathrm{h} - T_\mathrm{b}) \cdot \exp\left(-\frac{K_\mathrm{h}}{\sqrt{Tt}} \cdot \alpha \cdot t\right) \tag{5.79}$$

For the *fibre cooling*:

$$T_\mathrm{y} = T_\mathrm{r} + (T_\mathrm{b} - T_\mathrm{r}) \cdot \exp\left(-\frac{K_\mathrm{h}}{\sqrt{Tt}} \cdot \alpha \cdot t\right) \tag{5.80}$$

The following dimensions are to be inputted:

$T_\mathrm{y}, T_\mathrm{h}, T_\mathrm{r}, T_\mathrm{b}$	in K or °C
Tt	in tex
α	in $\mathrm{W/(m^2 \cdot K)}$
t	in s
K_h	as numerical value $5.9 \cdot 10^{-2}$ for PA
	as numerical value $7.6 \cdot 10^{-2}$ for PET

The value of $1.12\,\mathrm{g/cm^3}$ (for PA) resp. $1.38\,\mathrm{g/cm^3}$ (for PET) for the material density ϱ, and the value of $1.884\,\mathrm{kJ/(kg{\cdot}K)}$ (for PA) resp. $1.256\,\mathrm{kJ/(kg{\cdot}K)}$ (for PET) for the specific heat capacity c have been used for the calculation of K_h. The latter is almost valid in the temperature range of $40\,°\mathrm{C} \leq T_\mathrm{y} \leq 100\,°\mathrm{C}$.

The data of the heat transfer coefficient α presents a certain problem for practical calculations. This depends strongly on the surrounding medium which participates in the heat transfer (for threads normally resting or moving air or metallic surfaces), on the surface quality of the thread and the metallic contact areas, on the thread velocity, on the thread fineness and at last also on the mean temperature level at which the heat transfer takes place. An (but not without any difficulties) experimental estimation is indispensable for more detailed investigations of special process stages [315].

From the literature and on the basis of own investigations it is possible to use the following ranges which are valid for PA and PET threads for calculations with a good exactness:

For the heat transfer in air:

$$\alpha = 50...200 \text{ W}/(\text{m}^2 \cdot \text{K})$$

For the heat transfer on metallic surfaces (for instance godets):

$$\alpha = 450...600 \text{ W}/(\text{m}^2 \cdot \text{K})$$

Greater values are valid in the tendency for finer threads and for higher velocities.

The velocity dependence of the heat transfer coefficient for the heat exchange between thread and air can also be given a relationship which is presented in [316]. This has been investigated experimentally as "air streams alongside of even, rough metallic surfaces" which is valid for velocities of $v > 5$ m/s and which also gives useful results for threads in an air stream too. The relationship has been used also in the technological example for Sect. 5.3.3 and to the calculation of the time constants and critical frequencies of Table 5.2. It is read as (converted into SI-units):

$$\alpha = 7.52 \cdot v^{0.78} \tag{5.81}$$

If v is inserted in m/s then α will be obtained in $\text{W}/(\text{m}^2 \cdot \text{K})$.

The time constant T_{ch} and the critical frequency f_{ch} which describe the heat transfer dynamic of a thread can be read from the exponent of the exponential function in Eqs. 5.79 and 5.80:

$$T_{\text{ch}} = \frac{\sqrt{Tt}}{\alpha \cdot K_{\text{h}}} \tag{5.82}$$

$$f_{\text{ch}} = \frac{\alpha \cdot K_{\text{h}}}{2\pi\sqrt{Tt}} \tag{5.83}$$

The appropriate numerical values are collected for the used PA- and PET-threads of the technological application example in Sect. 5.3.3. The heat transfer coefficient for the heat transfer thread-metallic surface was taken as a basis of $\alpha = 530 \text{ W}/(\text{m}^2 \cdot \text{K})$.

The heat transfer coefficient α for the heat transfer moved thread-air has been selected depending on the velocity according to Eq. 5.81 and K_{h} for PA and PET according to the data of Eqs. 5.79 and 5.80.

Qualitative conclusions to the dynamic transmission behaviour are possible by aid of the general explanations in Sect. 4.2.1 (specifically statements dealing with Eq. 4.41). Each heat area- or air-contact with another temperature than T_{y} means an imprinting step for the thread. The explanations to the dynamic transfer functions with proportional action and delay of first order are analogously valid here.

Table 5.2. Time constants T_{ch} and critical frequencies f_{ch} of PA- and PET-threads corresponding to Eqs. 5.82 and 5.83

Material	Fineness Tt [tex]	Velocity v [m/min]	Time constant T_{ch} [s]	Critical frequency f_{ch} [Hz]
Heating or cooling of the thread in contact with a metallic surface:				
PA	5		$7.53 \cdot 10^{-2}$	2.11
PA	10		$1.07 \cdot 10^{-1}$	1.49
PA	20		$1.51 \cdot 10^{-1}$	1.06
PET	5		$5.55 \cdot 10^{-2}$	2.87
PET	10		$7.85 \cdot 10^{-2}$	2.03
PET	20		$1.11 \cdot 10^{-1}$	1.43
Heating or cooling of the thread in contact with surrounded air:				
PA	5	500	1.02	$1.57 \cdot 10^{-1}$
PA	5	1000	$5.92 \cdot 10^{-1}$	$2.69 \cdot 10^{-1}$
PA	5	2000	$3.45 \cdot 10^{-1}$	$4.62 \cdot 10^{-1}$
PA	5	3000	$2.51 \cdot 10^{-1}$	$6.34 \cdot 10^{-1}$
PA	5	4000	$2.01 \cdot 10^{-1}$	$7.93 \cdot 10^{-1}$
PA	10	500	1.44	$1.11 \cdot 10^{-1}$
PA	10	1000	$8.37 \cdot 10^{-1}$	$1.90 \cdot 10^{-1}$
PA	10	2000	$4.87 \cdot 10^{-1}$	$3.27 \cdot 10^{-1}$
PA	10	3000	$3.55 \cdot 10^{-1}$	$4.48 \cdot 10^{-1}$
PA	10	4000	$2.84 \cdot 10^{-1}$	$5.61 \cdot 10^{-1}$
PA	20	500	2.03	$7.83 \cdot 10^{-2}$
PA	20	1000	1.18	$1.35 \cdot 10^{-1}$
PA	20	2000	$6.89 \cdot 10^{-1}$	$2.31 \cdot 10^{-1}$
PA	20	3000	$5.02 \cdot 10^{-1}$	$3.17 \cdot 10^{-1}$
PA	20	4000	$4.01 \cdot 10^{-1}$	$3.97 \cdot 10^{-1}$
PET	5	500	$7.49 \cdot 10^{-1}$	$2.13 \cdot 10^{-1}$
PET	5	1000	$4.36 \cdot 10^{-1}$	$3.65 \cdot 10^{-1}$
PET	5	2000	$2.54 \cdot 10^{-1}$	$6.27 \cdot 10^{-1}$
PET	5	3000	$1.85 \cdot 10^{-1}$	$8.60 \cdot 10^{-1}$
PET	5	4000	$1.48 \cdot 10^{-1}$	1.08
PET	10	500	1.06	$1.50 \cdot 10^{-1}$
PET	10	1000	$6.16 \cdot 10^{-1}$	$2.58 \cdot 10^{-1}$
PET	10	2000	$3.59 \cdot 10^{-1}$	$4.43 \cdot 10^{-1}$
PET	10	3000	$2.62 \cdot 10^{-1}$	$6.08 \cdot 10^{-1}$
PET	10	4000	$2.09 \cdot 10^{-1}$	$7.61 \cdot 10^{-1}$
PET	20	500	1.50	$1.06 \cdot 10^{-1}$
PET	20	1000	$8.72 \cdot 10^{-1}$	$1.83 \cdot 10^{-1}$
PET	20	2000	$5.08 \cdot 10^{-1}$	$3.13 \cdot 10^{-1}$
PET	20	3000	$3.70 \cdot 10^{-1}$	$4.30 \cdot 10^{-1}$
PET	20	4000	$2.96 \cdot 10^{-1}$	$5.38 \cdot 10^{-1}$

5.3.3 Technological Application Examples

Dynamics of Fibre Heating of Man-Made Fibres at Heated Godet Systems

The presented technological schemes of a heated godet roll duo (arrangement I, following abbreviated with A I) and a heated godet roll with unheated temple pulley (arrangement II, following abbreviated with A II) are taken as the basis for the following investigations (see Fig. 5.31). These arrangements could be realised for instance at the spin-draw-winding process (SDW-process). The example rests essentially upon already published results of a formerly revised paper ([317]).

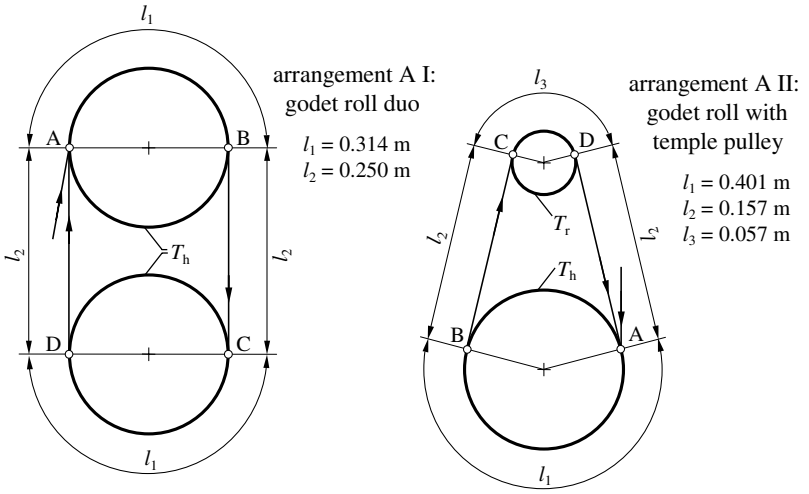

Fig. 5.31. Arrangements of heated godets

The following short signs have been chosen corresponding to Sect. 5.3.2:

T_b	thread temperature at the input into the godet arrangement
T_r	temperature of the cool medium, that means both the surrounding air temperature and the temperature of the unheated temple pulley corresponding to A II
T_h	temperature of the heated godet surface
$T_1, T_2, ...T_n$	thread temperatures
T_y	after passing the single heating and cooling lines
α_1	heat transfer coefficient between metallic surface and thread (for heating and cooling assumed of the same quantity)
α_2	heat transfer coefficient between air and thread
l_1	contact line of the thread with the heated godet surface

	(for A I and A II differently long corresponding to the different geometry of the thread way around the godet arrangements, see Fig. 5.31)
l_2	air line of the thread (for A I and A II differently long corresponding to the different geometry of the thread way around the godet
l_3	contact line of the thread with the surface of the unheated temple pulley
Tt	thread fineness
K_h	thread material specific constant for the heat transfer (definition see Sect. 5.3.2)
v	thread velocity
z	number of thread wraps around the geometric arrangement (one wrap = length of the way $\overline{\mathrm{ABCDA}}$)

The basis for the calculation is the common DEq. for the heat transfer 5.73 and its solutions 5.79 and 5.80 (step responses) for heating and cooling. The equation system reads for a full thread wrap around the godet arrangement A I (heated godet roll duo) corresponding to these derived basic equations ($l_1 ... l_3$ are to be put in m, v is to be put in m/s, the other quantities are to be put in as upper defined):

$$T_1 = T_\mathrm{h} - (T_\mathrm{h} - T_\mathrm{b}) \cdot \exp\left(-\frac{K_\mathrm{h} \cdot l_1 \cdot \alpha_1}{v \cdot \sqrt{Tt}}\right) \tag{5.84}$$

$$T_2 = T_\mathrm{r} + (T_1 - T_\mathrm{r}) \cdot \exp\left(-\frac{K_\mathrm{h} \cdot l_2 \cdot \alpha_2}{v \cdot \sqrt{Tt}}\right) \tag{5.85}$$

$$T_3 = T_\mathrm{h} - (T_\mathrm{h} - T_2) \cdot \exp\left(-\frac{K_\mathrm{h} \cdot l_1 \cdot \alpha_1}{v \cdot \sqrt{Tt}}\right) \tag{5.86}$$

$$T_4 = T_\mathrm{r} + (T_3 - T_\mathrm{r}) \cdot \exp\left(-\frac{K_\mathrm{h} \cdot l_2 \cdot \alpha_2}{v \cdot \sqrt{Tt}}\right) \tag{5.87}$$

The equation system reads for a full thread wrap around the godet arrangement A II (heated godet with unheated temple pulley) as:

$$T_1 = T_\mathrm{h} - (T_\mathrm{h} - T_\mathrm{b}) \cdot \exp\left(-\frac{K_\mathrm{h} \cdot l_1 \cdot \alpha_1}{v \cdot \sqrt{Tt}}\right) \tag{5.88}$$

$$T_2 = T_\mathrm{r} + (T_1 - T_\mathrm{r}) \cdot \exp\left(-\frac{K_\mathrm{h} \cdot l_2 \cdot \alpha_2}{v \cdot \sqrt{Tt}}\right) \tag{5.89}$$

$$T_3 = T_\mathrm{r} + (T_2 - T_\mathrm{r}) \cdot \exp\left(-\frac{K_\mathrm{h} \cdot l_3 \cdot \alpha_1}{v \cdot \sqrt{Tt}}\right) \tag{5.90}$$

$$T_4 = T_\mathrm{r} + (T_3 - T_\mathrm{r}) \cdot \exp\left(-\frac{K_\mathrm{h} \cdot l_2 \cdot \alpha_2}{v \cdot \sqrt{Tt}}\right) \tag{5.91}$$

The heating process similarly pursues the 2^{nd}, 3^{rd}, ... , n^{th}-wrap. The, in each case, actual thread temperatures T_1, T_2, ..., T_n are only to be taken over in the next following exponential equations which describe the next heating or cooling line of the thread.

In principle Fig. 5.32 shows the course of the heating process for both arrangements A I and A II. The end values of the e-functions (which the thread temperature T_y passes through the single thread lines) are connected simply by straight lines. The thread way l_y corresponds to the sizes of the geometrical godet arrangements which were the basis for the investigations. This thread way l_y is of course proportional to the running time t if the thread velocity is constant.

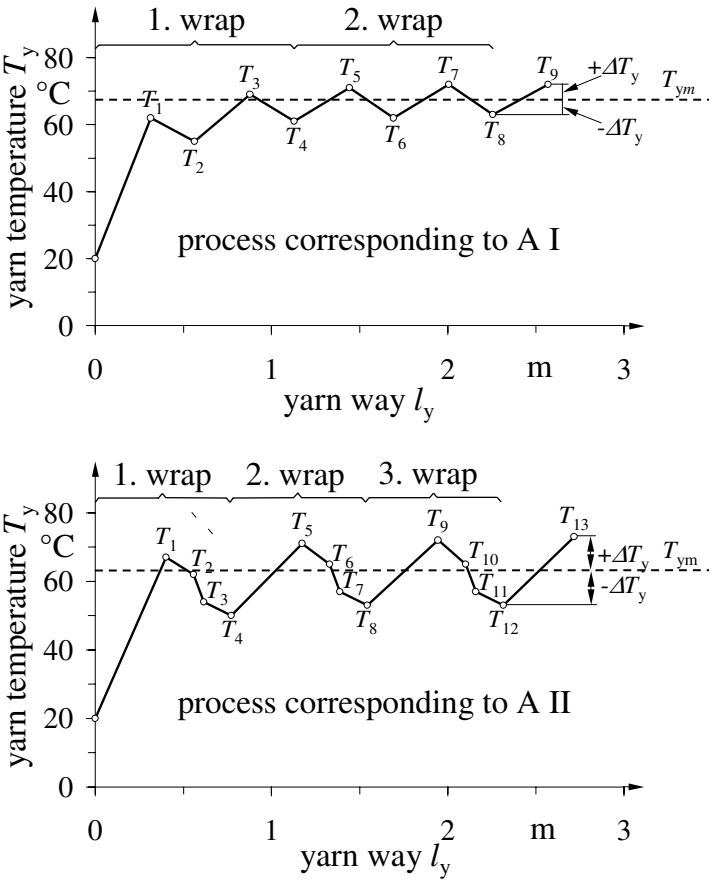

Fig. 5.32. Course of principle of thread heating on heated godet arrangements corresponding to Fig. 5.31

It can be seen by using the Eqs. 5.84 to 5.91 that the total heating process is only reproducible by means of a system of inputting each other and dependent on each other e-functions. It appears that the system behaviour can be described sufficiently by means of the following four aim quantities:

a) minimum number of thread wraps z
The quantity z is the minimum number of thread wraps which is necessary to reach the steady state condition of the heating and cooling process at a determined technological variant (Fig. 5.33). This has been defined in the calculation program by means of a breaking off criterion. The steady state condition is reached accordingly if the difference of the yarn temperatures at the end of both last calculated heating sections falls below which is a limit value, occurring for the first time, and which is given odds at your convenience. One K has been chosen as the limit value in the following numerical examples.

b) mean value of the thread temperature T_{ym}
T_{ym} means the mean value of the yarn temperature T_{y} (Fig. 5.34). The latter oscillates around T_{ym} after the steady state condition has been reached:

$$T_{\mathrm{ym}} = \frac{T_{\mathrm{n}} + T_{\mathrm{n-1}}}{2} \tag{5.92}$$

T_{n} is on this occasion the yarn temperature at the end of the last heating section at which the breaking off criterion has been reached, occurring for the first time.

c) relative thread temperature oscillations $\Delta T_{\mathrm{y}}/T_{\mathrm{ym}}$
The relative thread temperature oscillation $\Delta T_{\mathrm{y}}/T_{\mathrm{ym}}$ is the percent oscillation range (as the $\pm$ quantity) of the thread temperature referring to its mean value T_{ym} (Fig. 5.35).

$$\frac{\Delta T_{\mathrm{y}}}{T_{\mathrm{ym}}} \cdot 100\% = \frac{T_{\mathrm{n}} - T_{\mathrm{n-1}}}{T_{\mathrm{n}} + T_{\mathrm{n+1}}} \cdot 100\% \tag{5.93}$$

d) heating yield η_{h}
η_{h} represents the ratio of the thread temperature mean value T_{ym} to the temperature of the godet surface T_{h} (Fig. 5.36).

$$\eta_{\mathrm{h}} = \frac{T_{\mathrm{ym}}}{T_{\mathrm{h}}} \cdot 100\% \tag{5.94}$$

η_{h} is also a measurement for the approximation of the yarn temperature to the theoretical maximum possible quantity T_{h}. The latter could only be reached by a sufficiently large number of yarn wraps if the cooling lines would be

reduced to zero. η_h is not in this respect a yield in the energy sense. Furthermore it is of course to be remarked that this quantity possesses only relative comparing character in case the temperatures are given (as usually) in ℃.

Calculation results are presented following for the aim sizes previously defined in a choice of diagrams (Figs. 5.33 to 5.36) for the yarn materials PA and PET with the finenesses Tt = 5, 10 and 20 tex. Temperatures of the heated godets in each case of T_h = 70℃ and 100℃ are assumed for both geometrical arrangements A I and A II according to Fig. 5.31. Heat transfer coefficients are taken as the basis as follows:

yarn - metallic surface: $\alpha_1 = 530\ \mathrm{W/(m^2 \cdot K)}$,
yarn - air: according to Eq. 5.81.

The systems have been investigated in the yarn velocity range of 500 to 4000 m/min (time constants and critical frequencies of these cases regarding heating and cooling see Table 5.2).

The following fundamental statements can be learned from the Figs. 5.33 to 5.36:

a) The minimum number of thread wraps z (which is necessary to reach the steady state yarn temperature state T_{ym}) is shown in Fig. 5.33. It must be higher, the higher the yarn velocity v, the coarser the heating yarn and the higher the godet temperature T_h. The arrangement A II enforces roughly 1.5 times more wraps than the arrangement A I, where PA enforces, on the average, a somewhat higher number of wraps than PET. It is remarkable that more than 10 wraps are necessary to reach the mean yarn temperature T_{ym} if coarser yarns are to be heated at higher velocities.

b) The mean yarn temperature T_{ym} (see Fig. 5.34) depends on the yarn velocity. T_{ym} decreases according to the expectation of higher velocity. This decrease amounts in the simulated range (dependent on the yarn fineness and the godet temperature) 15 ... 25℃! The reached temperatures at smaller velocities ($v < 1000$ m/min for PA, $v < 1500$ m/min for PET) are significantly higher at the arrangement A I (godet roll duo) than at the arrangement A II. This tendency is obliterated at higher velocities ($v > 2000$ m/min) in so-far as (dependent upon the yarn fineness) the A II (godet roll with a temple pulley) can produce the somewhat higher mean yarn temperatures. The fineness influence comes forth clearly at higher velocities for both arrangements: Coarser yarns can be heated to a lower mean temperature compared to finer yarns. The difference can amount to $v = 4000$ m/min at 10℃ (5 tex compared with 20 tex). It is also remarkable that PET-yarns can be heated to higher temperature (especially at higher yarn velocities) on the average than PA-yarns under the same technological boundary conditions and despite

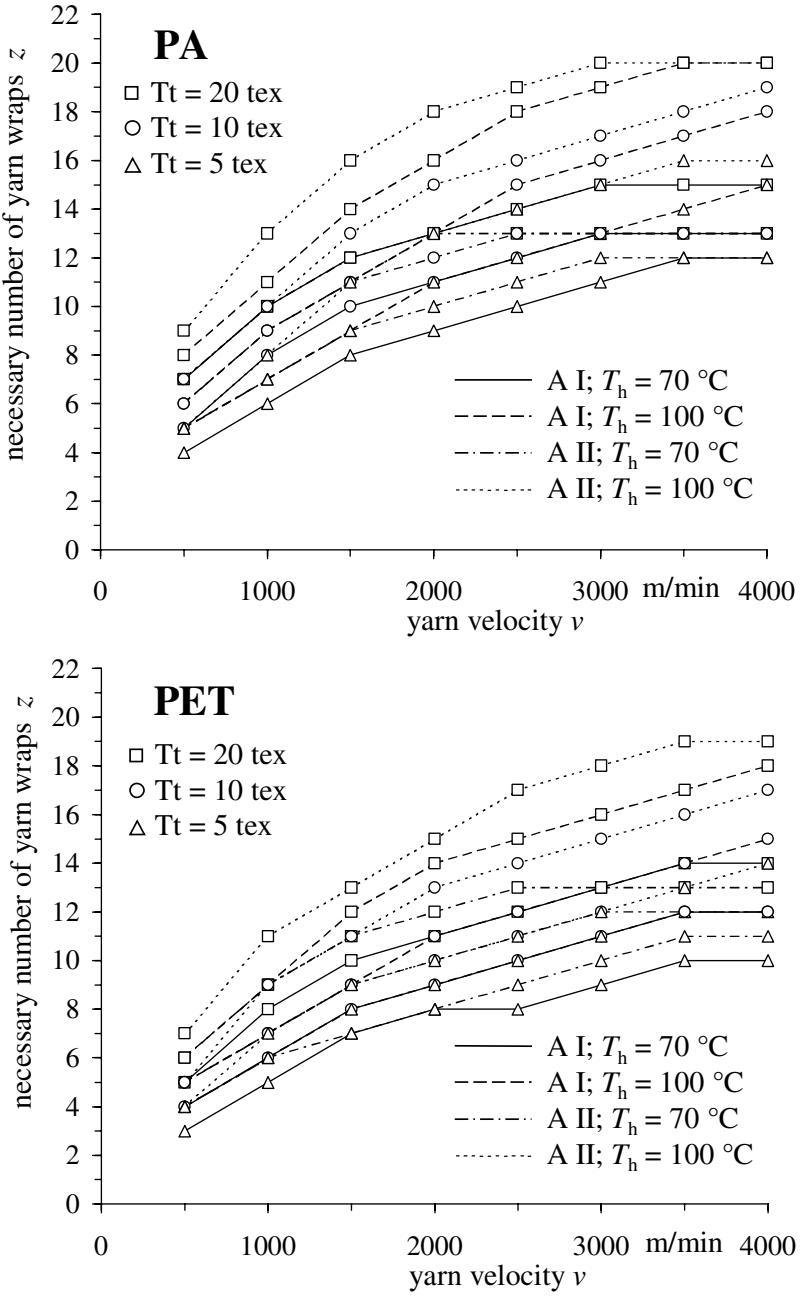

Fig. 5.33. Necessary numbers of thread wraps z around heated godet arrangements A I and A II, corresponding to Fig. 5.32

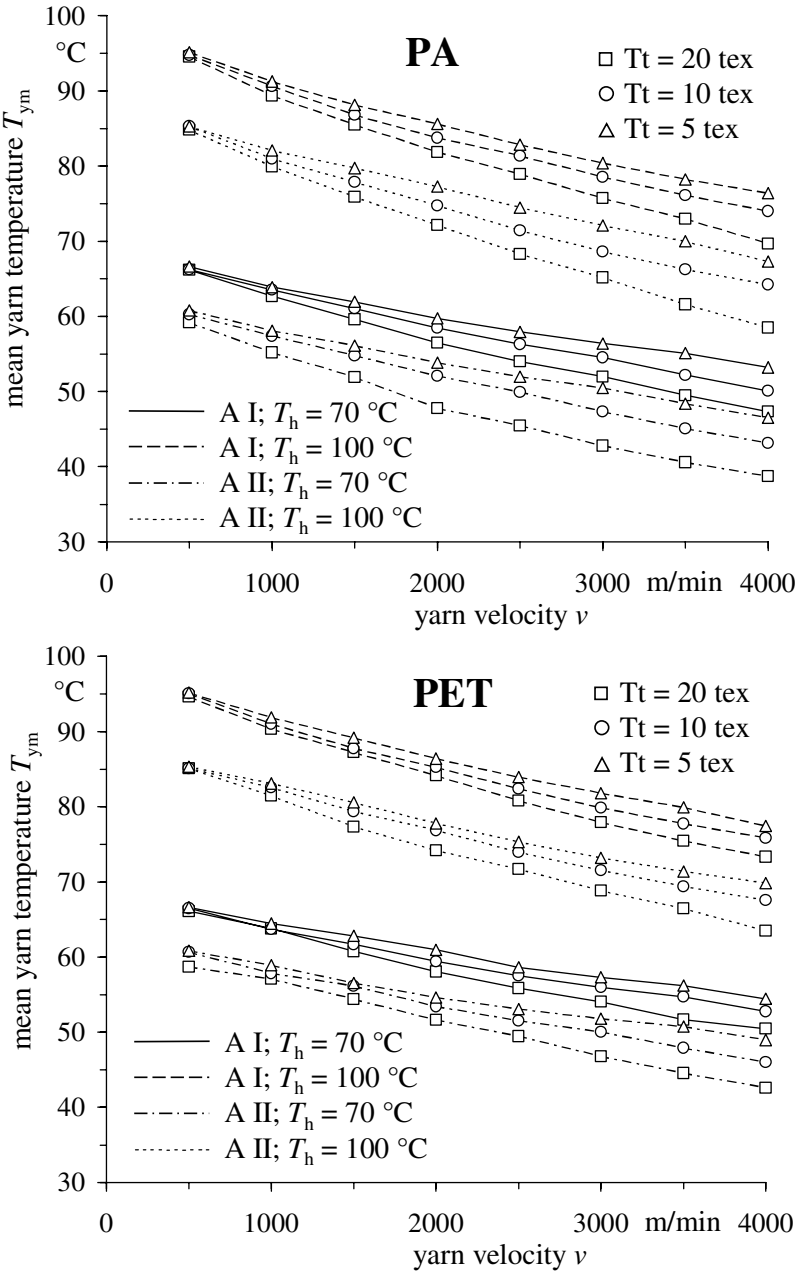

Fig. 5.34. Mean values of the thread temperatures T_{ym} at the thread running around heated godet arrangements A I and A II, corresponding to Fig. 5.32

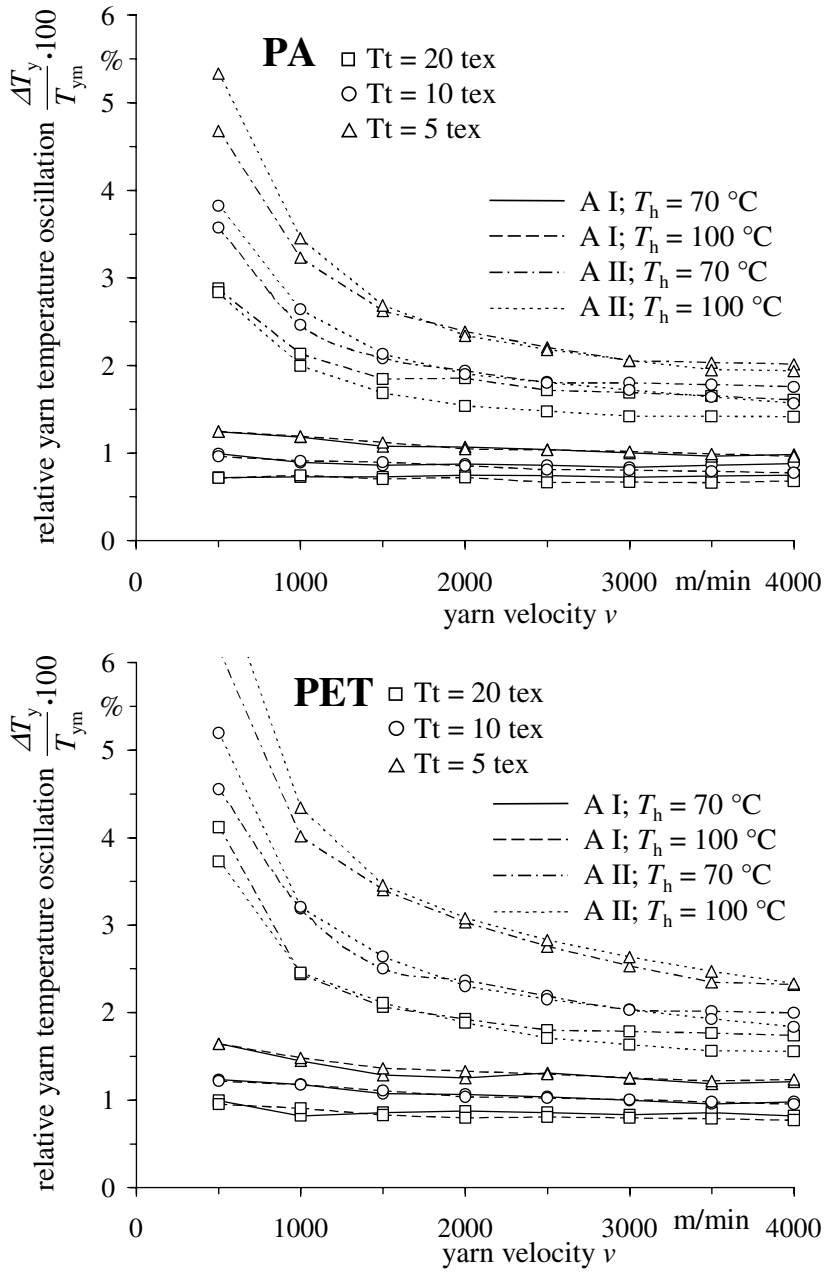

Fig. 5.35. Relative thread temperature oscillations $\Delta T_y/T_{ym}$ at the running around heated godet arrangements A I and A II, corresponding to Fig. 5.32

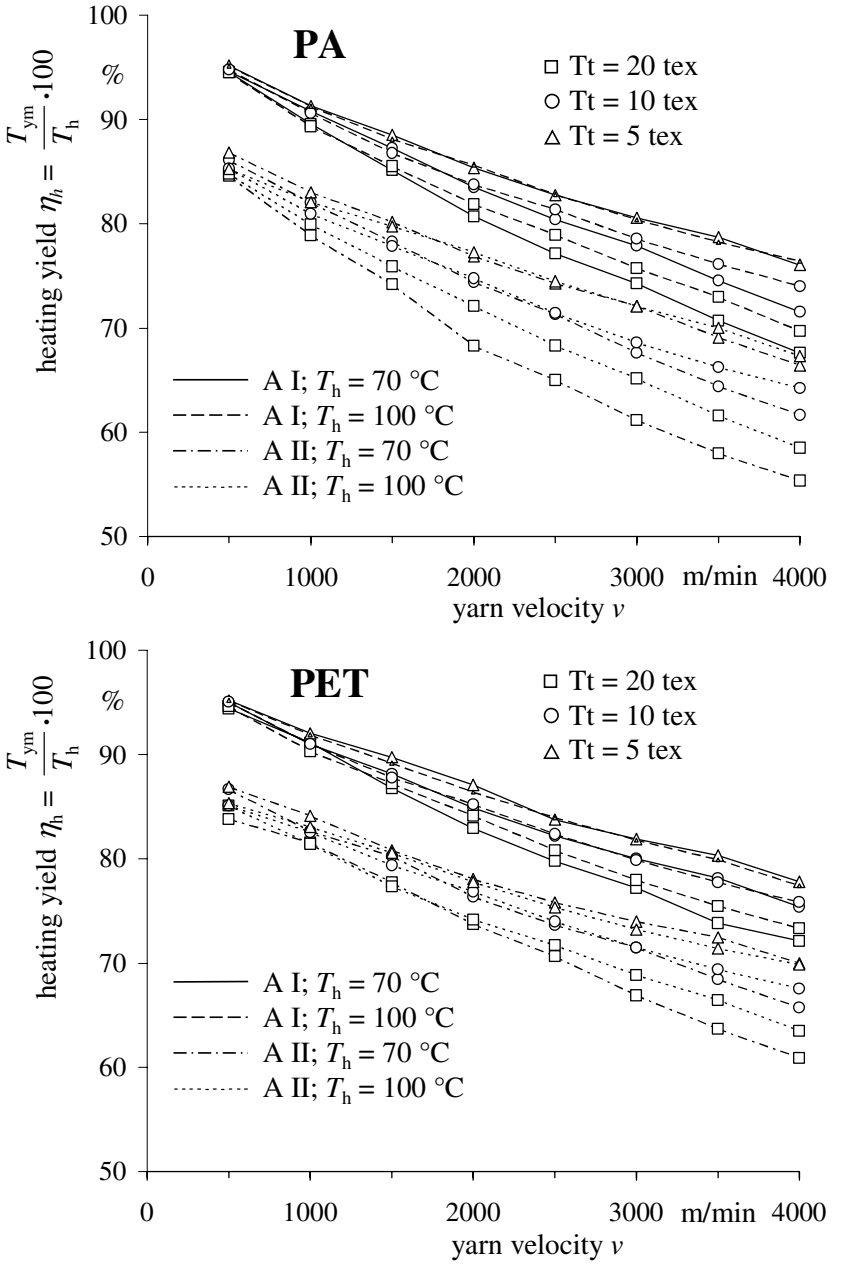

Fig. 5.36. Heating yield η_h at the thread running around heated godet arrangements A I and A II, corresponding to Fig. 5.32

the same godet temperatures. Nevertheless, the relative dependences are the same for both yarn materials.

It is quantitatively shown with these calculations that in principle the mean yarn temperatures cannot reach the temperature of the heated godet surface at such godet arrangements: The used godet temperatures will fail in the yarn (at $v = 4000$ m/min) for instance between 20 and 40 ℃ for PA and between 15 and 30 ℃ for PET. A difference of 5 to 15 ℃ can be seen even at $v = 500$ m/min to the theoretically possible value T_{h}.

c) A very important aim quantity is the relative yarn temperature oscillations $\Delta T_{\mathrm{y}}/T_{\mathrm{ym}}$ about the mean yarn temperature T_{ym} which the yarn suffers at each full wrap around the godet systems (see Fig. 5.35). This enormous temperature change stress is imprinted onto the yarn in the investigated velocity range nevertheless between 15 and 110 times/s, also with a disturbance frequency of 15 to 110 Hz!

The following tendencies can be read as:
The temperature change stress decreases with increasing velocity, coarser yarns and decreasing temperature of the heated godets. The arrangement A II strains the yarn more than the arrangement A I. Change stresses up to ±5 ℃ can be awaited specifically in the range of small velocities (< 1000 m/min) for finer yarns at the higher godet temperature ($T_{\mathrm{h}} = 100$ ℃). The dampening effect (which is correlated with the critical frequency of the system "to heating or to cooling thread") is effective in higher degrees ($f > f_{\mathrm{ch}}$) for the higher velocities, this means for higher disturbance frequencies. The temperature change stress of the yarn decreases to uncritical values of $< 2\%$ (see also time constants and critical frequencies in Table 5.2). The yarn material PET is exposed to a somewhat greater temperature change stress than the yarn mateial PA under the same technological conditions.

d) If one looks at the heating yield η_{h} (see Fig. 5.36) then a clear decrease is to be noticed above all with increasing yarn velocity. The tendencies are confirmed which are named under a): A I is more favourable, on the average, according to the heat transfer (two heated godets are necessary, compared to only one at A II!). But, this is no longer valid for coarser yarns (which generally have the worse heat transfer conditions) at high yarn velocities. PET-yarns can be heated with a higher heating yield η_{h} than PA-yarns.

Fibre Cooling in the Melt Spinning of Polymers (simplified)

Extensive investigations to the modelling and the complex proceedings in the fibre formation distance have been described in detail in Sects. 3.1. and 3.2. One of the most important product variables is the temperature of the melt stream T_{f} which withdraws from the spinning die and solidifies along the spinning way l_{s} in the last amount of time to the filament with the fineness

Tt_f. This problem is not able to be solved by means of the developed equations in Sect. 5.3.2, but it is also pronounced as a problem of the thread cooling dynamic. In the following it should be made clear that calculation results describe the cooling process in a modified manner. These are based on the application of a simple to handle basic equation which has been developed in a formerly restricted paper the modelling of the fibre formation in melt spinning [280]. It is taken into account at this occasion that the heat transfer conditions and the heat capacity c of the solidifying polymer melt is subjected to greater temperature depending changes. The following result (based on the concentration of experimental data) is explained in [280]: The quotient of the specific heat capacity c and the NUSSELT-number[3] is roughly constant along the whole spinning way l_s. An analytical equation can be derived on the basis of this knowledge (after some intermediate steps which are not performed here) for the temperature course of the formated filament is as follows:

$$T_f = T_r + (T_s - T_r) \cdot \exp(l_s/x_0) \tag{5.95}$$

The length measurement x_0 can be calculated as follows:

$$x_0 = 1.5 \cdot K_{W1} \cdot (q_o)^{0.79} \cdot (v_s)^{-0.05} \tag{5.96}$$

or

$$x_0 = 1.5 \cdot K_{W2} \cdot (Tt_f)^{0.79} \cdot (v_s)^{0.74} \tag{5.97}$$

The single sizes and their dimensions in Eqs. 5.95 to 5.97 mean:

T_f	filament temperature in °C or K
T_r	temperature of the cooling medium (surrounding air) in °C or K
T_s	temperature of the spinneret = melt temperature at the spinneret output in °C or K
l_s	distance from the spinneret = spinning way in m
x_0	length measurement corresponding to Eqs. 5.96 or 5.97, dimension reads in m
q_o	throughput of one orifice in the spinneret = filament throughput in g/min
Tt_f	fineness of the filament
v_s	spinning velocity in m/min
K_{W1}	polymer-specific constant in Eq. 5.96 K_{W1}=0.81 for PA K_{W1}=0.57 for PET K_{W1}=0.91 for PP

[3] The NUSSELT-number is a dimensionless quantity to the description of the heat transfer which arises from the heat transfer coefficient α, the heat conductivity λ of the surrounding medium and a characteristic length measurement d as follows: $Nu = \alpha \cdot d/\lambda$.

K_{W2} polymer-specific constant in Eq. 5.97
$K_{W2} = 3.44 \cdot 10^{-3}$ for PA
$K_{W2} = 2.42 \cdot 10^{-3}$ for PET
$K_{W2} = 3.89 \cdot 10^{-3}$ for PP

Equation 5.95 also describes the filament temperature course depending on the distance from the spinneret, that means on the spinning way l_s. The knowledge of this dependence is specifically important for the best design of the spinning tube length or for the placing of filament treatment elements in the filament line (for instance preparation disk or preparation finger).

Some typical filament temperature courses are shown in Fig. 5.37 for the most important spinning materials PA and PET. Spinning velocities v_s of 1000, 4000 and 6000 m/min and finenesses of the spun filaments Tt_f of 1 and 0.3 tex for both materials have been chosen. The spinneret temperature T_s has been set at 280℃ for PA and 300℃ for PET. The temperature of the cooling medium (surrounding air) $T_r = 20$℃ and the diameter of the orifice $d_o = 0.25$ mm (which is not of any effect) have been constantly chosen.

Quantitative tendencies of the cooling behaviour and conclusions in different directions can be easily learned using the single curves from this diagram. It can be seen as a quantitative completion of Sect. 3.1.7.

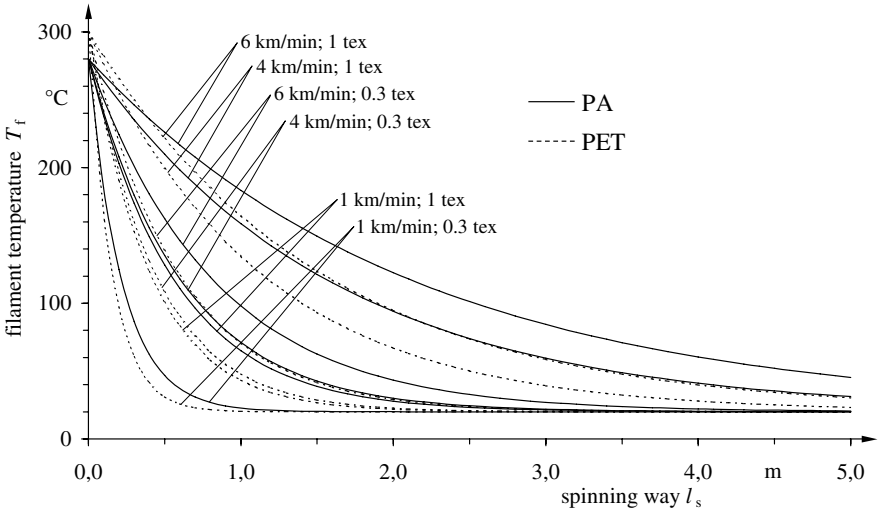

Fig. 5.37. Filament temperature courses T_f dependent upon the spinning way l_s in the melt spinning of polymers